

1 Introduction

This chapter aims to cover theoretical and computational studies on organometallic molecules. Section 1 covers the s and p-block elements and Section 2 covers the d- and f-block metals. Clusters, carbonyls and metal-metal bonded systems containing M-C bonds are included. Extended systems and organic species on metal surfaces are excluded except where calculations have been performed on model complexes designed to mimic solid state and surface chemistry.

A wide variety of computational methods is employed in the computational chemistry community. As in previous recent years, density functional theory (DFT) continues to grow in prominence. The vast majority of the work described in this chapter has been performed at the DFT level with the hybrid functional B3LYP being the most popular for studies of organometallic molecules and reactions. ‘Traditional’ *ab initio* approaches including Hartree-Fock (HF) and post-HF methods (including MP2 and MP4) continue to be used, often for comparison with DFT based methods. Semi-empirical methods now appear to have only limited use except in the molecular mechanics (MM) calculations. A relatively new use of molecular mechanics for large systems is in hybrid calculations where the transition metal and its coordination environment or the reactive centre of a molecule are treated at a higher level leaving the remainder to be treated at the MM level. These QM/MM or ONIOM calculations enable the steric bulk of organometallic molecules to be adequately but computationally efficiently treated and are becoming particularly prevalent in studies of reaction mechanisms and profiles.

Only a brief mention of the computational method is given. Standard abbreviations for computational methods are employed throughout. Given the plethora of basis sets available in modern computational chemistry programs and the variety of basis set designations employed by authors in this field, no description of basis sets is given. The reader should consult the original work for further details of the computational method and the basis set.

2 s- and p-Block Metals

2.1 Structural and Spectroscopic Studies. – *2.1.1 Metal Alkyls and Analogues.* A B3LYP and AIM study¹ of the electron density on the ethyl ligand and related organic groups in alkyllithium complexes reveals charge concentrations in the valence shell at the α and β -atoms suggesting delocalization of the lone pair at the α -C atom or of the Li-C bonding electrons. As a consequence, it is suggested that Li . . . H contacts are due to this delocalization, with Li . . . H agostic interactions playing only a minor role. The equilibrium between Al atoms, trimethylaluminum and an Al-TMA complex is predicted by B3LYP and MP2 calculations² to lead to a complex which contains an Al-Al bond semi-bridged by a methyl group.

The structure of the GaMe₃ dimer, optimized at the MP2 level³, is very similar that found in the tetragonal solid. CIS and TDDFT calculations⁴ on dimethylstannylene, SnMe₂, have been used to assign absorption spectrum of the products of the flash photolysis of SnMe₄. The S-bound methyl groups in (Me₂MCH₂SMe)₂ complexes (M = Al, Ga, In) are placed in equatorial positions of the chair-like six-membered ring systems with the conformation with both S-Me groups in axial positions being higher in energy by *ca.* 25 kJ mol⁻¹, according to MP2 and B3LYP calculations⁵. The HeI photoelectron spectra of trimethylaluminum, triethylaluminum, dimethylaluminum, and diethylaluminum hydrides have been interpreted with the aid of *ab initio* quantum chemical calculations, including Hartree-Fock/Koopmans, outer valence Green's function, and equation of motion coupled-cluster ionization energy calculations⁶. Luminescence from the novel blue phosphorescent Group 15 compounds MR₃ (M = P, Sb, Bi; R = p-(N-7-azaindoly)phenyl) are ligand-based emissions with contributions from the lone-pair electrons of the central atom, a Hartree-Fock study has revealed⁷.

The structures, vibrational frequencies and barriers to internal rotation of the MX₃ group in CH₂=CH-MX₃ (M = C, Si, and Ge; X = F and Cl) compounds have been investigated at the B3LYP and MP2 levels⁸. A decrease in the MX₃ rotational barrier in the order C > Si > Ge is predicted and is attributed to the decrease in the C-M covalent bond character. Dissociation energies and structures of the donor-acceptor adducts Et₃Al-E(SiMe₃)₃ and ^tBu₃Al-E(ⁱPr)₃ (E = P, As, Sb, Bi) have been studied at the B3LYP level⁹. The thermodynamic stability of these depends both on the electronic strength of the Lewis acid and base, which is influenced by the central Group 13 and 15 elements, their substituents, and on steric interactions between the Lewis acid and base. B3LYP calculations¹⁰ on carbochalcogenoates CH₃COEM(CH₃)₃ complexes (E = Se, Te; M = Ge, Sn, Pb) show a shortening of the C=O . . . Sn distances compared to the C=O . . . Ge bonds due to greater oxygen lone pair → M-E σ^* donation. MP2 calculations¹¹ on Cl₃Te[CH₂CH(Cl)CH₂O(H) . . .] and Cl₃Te[CH₂CH(CH₂Cl)OC(CH₃)=O . . .] reveal strong oxygen lone pair → σ^* (Te-Cl) and Coulombic interactions for the Te . . . O bonds, leading to significantly longer bonds in the isolated molecules than in the solid state. The structures of the C, Si and Ge analogues of the perfume ingredient majantol [2,2-dimethyl-3-(3-

methylphenyl)propan-1-ol] have been determined at the RI-MP2 level¹². The ¹¹⁹Sn isotropic chemical shifts for the grouping C-N-Sn(CH₃)₃-N-C, characteristic of a series of solid organometallic compounds have been calculated at the B3LYP level¹³ revealing a strong influence on the Sn-N-C bond angle.

The molecular structures of methylaluminumoxanes with three-coordinated aluminium centres, calculated at HF, MP2 and B3LYP levels¹⁴, are determined by the strain due to ring formation and/or by the stabilizing π -bonding interactions between the oxygen lone pairs and vacant p-orbitals of the metals. The silanes Me₂Si(CR'R₂)(CR''R₂) (R = H, R'' = Me and R' = R'' = Me, CR₂ = fluorenyl) and Me₂Si(CHR₂)₂ exhibit extensive intramolecular and intermolecular C-H... π interactions leading to supramolecular associations, according to AMI semi-empirical molecular orbital calculations¹⁵.

The isotropic shielding of the tin nucleus in the reference compound tetramethyltin and a series of tetra-organotin compounds have been calculated at the B3LYP level¹⁶ to examine the effects of varying ligand chain-length, substitution at the α and β positions and bond order for compounds of the type Me₃SnR. The trimeric diphenyltin chalcogenides (Ph₂SnS)₃ have twisted boat conformations as the global minimum at the B3LYP level¹⁷. B3LYP calculations¹⁸ suggest that the barrier to inversion of the monomer of 2-lithio-N-formylpyrrolidine is increased by use of non-coordinating solvents but lowered by aggregation into a trimer.

2.1.2 Clusters. The geometries and thermodynamic properties of twenty-four Group 13-Group 16 chalcogen heterocubanes [RM(μ^3 -E)]₄ (R = H, CH₃; M = Al, Ga, In; E = O, S, Se, Te) and twelve Group 13-Group 13 pure cubanes [RM(μ^3 -M)]₄ (R = F, Cl, CH₃, NO₂; M = Al, Ga, In) have been studied at the B3LYP level¹⁹. The chalcogen heterocubanes are predicted to be thermodynamically resistant to fragmentation. B3LYP calculations²⁰ on the Na₂[CAL₄]₂ dimer predict that structures with a C-C bond are higher in energy than the structures with two isolated structural [CAL₄]⁻ units. Formation of a [C₂Al₈]⁴⁻ cluster without a C-C bond are only slightly higher in energy. The structures and bonding of the closo-[1-M(CO)₅(μ^4 -E₉)]⁴⁻ (E = Sn, Pb; M = Mo, W) cluster anions have been studied at the DFT level²¹. The three-dimensional aromaticity of [(AlH)₆(AlNMe₃)₂(CCH₂R)₆] (R = Ph, CH₂SiMe₃) has been investigated using *ab initio* and Hückel calculations²² suggesting that each Al₄C fragment of the cube is formed by four bonds with three electron pairs, thus leading to a strong delocalization of the electrons. B3LYP calculations²³ have been used to study the bonding in Al metalloid clusters including [Al₇{N(SiMe₃)₂}]₆⁻, [Al₁₂{N(SiMe₃)₂}]₈⁻, [Al₂₂Br₂₀•12THF], Al₁₄{N(SiMe₃)₂}]₆I₆]²⁻, Al₁₄(μ_8 -Si)Cp*₆, [(AlEt)₈(μ_4 -CCH₂Ph)₅(μ_4 -H)], [(AlMe)₈(μ_4 -CCH₂Ph)₅(μ_4 -CCPh)] and [(AlMe)₇(μ_4 -CCH₂Me)₄(μ_2 -H)₂] and show the relationship between the observed geometry and electron counts.

Increasing the proton donor ability of acids leads to the formation of bifurcate H-bonds in the complexes [B₁₀H₁₀]²⁻•HOCH₃, [B₁₀H₁₀]²⁻•HOCF₃, [B₁₀H₁₀]²⁻•HCN, and [B₁₂H₁₂]²⁻•HOCH₃ complexes, a HF study²⁴ reveals, in agreement with experimental observations. The colour of the pyridine-containing azanaboranes [(C₅H₅N)B₈H₁₁NHR] (R = methyl, ethyl, isopropyl or tertiary

butyl) is strongly dependent on the energy of the LUMO which is itself strongly influenced by the π -donor ability of the substituent, an AM1 study reveals²⁵. A B3LYP study²⁶ suggests that the macropolyhedral thiaboranes $[\text{S}_2\text{B}_{17}\text{H}_{17}\text{-SMe}_2]$ and $[\text{S}_2\text{B}_{18}\text{H}_{19}]^-$ do not form for kinetic reasons only.

The hexacoordinated tin atoms in the nanocluster $[(\text{CH}_3\text{Sn})_{12}\text{O}_{14}(\text{OH})_6]^{2+}$ are harder than the pentacoordinated tin atoms according to a B3YLP and HF study²⁷. Molecular electrostatic potential calculations indicate that nucleophiles will approach preferentially the macrocation around the poles rather than at the equator of the cage.

2.1.3 Cyclopentadienyl Complexes and Analogues. Recent developments in the chemistry of cyclopentadienyl derivatives of the alkaline-earth metals, including computational studies, have been reviewed^{28,29}. The geometries, metal-ligand bond dissociation energies, and heats of formation of twenty sandwich and half-sandwich complexes of the main-group elements of Groups 1, 2, 13, and 14, and Zn have been calculated at the BP86 and CCSD(T) levels³⁰ and the nature of the metal-ligand bonding analysed with an energy-partitioning method.

The structure and anisotropic NMR interaction tensors in the bis (penta-methyl cyclopentadienyl) aluminum cation, $[(\text{Cp}_2\text{Al})]^+$ have been calculated using RHF and B3LYP computations and the GIAO method³¹. There is a low barrier to rotation of the rings. The orientations of the NMR tensors, the large chemical shielding span, and the very small value of $C_Q(^{27}\text{Al})$ can all be rationalized in terms of the high molecular symmetry. The orthorhombic zigzag phase of plumbocene, $\text{Pb}(\text{C}_5\text{H}_5)_2$ is lower in energy than a lattice comprising uniformly staggered rings by 2.8 kJ mol^{-1} due to the difference in the strength of intermolecular interactions between the chains for the two different lattices, according to plane-wave DFT calculations³².

2.1.4 Carbonyls. B3LYP calculations³³ of the structure and IR spectrum of the boron carbonyl $(\text{CF}_3)_3\text{BCO}$ confirm its experimental formation and indicate that it has a bond strength of *ca.* 110 kJ mol^{-1} . B3LYP calculations³⁴ confirm experimental observations of the neutral OCBBCO molecule and suggest that it has a linear singlet ground state with a very short boron-boron bond length, indicative of a unusual boron-boron triple bond. Calculation of the vibrational spectrum at the B3LYP level³⁵ confirms that reaction of PhSiMe with CO yields the carbonyl complex $\text{PhSi}(\text{CO})\text{Me}$. MR-CI calculations³⁶ on Sr^+CO reveal the existence of a bistable species with strontium either bonded to the carbon-end or to the oxygen-end of CO in collinear geometries.

3.1.5 Low Valent and Multiply Bonded Systems. Computational and experimental studies³⁷ of Group 13 complexes, containing M(0), M(I) and M(II) including MCO, MCH_3 and HMCH_3 , and complexes of M_2 with substrates such as H_2 , CO, N_2 , CH_4 , NH_3 and PH_3 , have been reviewed. Computational studies of homonuclear triple bonding between heavier Group 14 elements have been reviewed³⁸. Acetylenes may behave either as acidic or basic probes, by virtue of the $\equiv\text{C-H}$ group, which is acidic, and of the $\text{C}\equiv\text{C}$ triple bond, which can interact

with positively charged centres, such as acidic hydroxyls or metal cations suggests a B3LYP study³⁹ of alkali metal cation - acetylene and methylacetylene interactions. The oxidation states and stabilities of group 13 carbene analogues [$\{HC(CR'NR'')_2\}E$] ($E = B, Al, Ga$ and In) have been investigated at the BP86 and B3LYP levels⁴⁰ suggesting that the In system should have similar stability to the experimentally known compounds of Al and Ga but that the B homologue is expected to be highly reactive. B3LYP calculations⁴¹ on the donor-acceptor complexes $R_3E-E'R'$ and the isomeric $R_2E-E'RR'$ complexes ($E, E' = B-Tl$ and $R, R' = H, Cl, CH_3$) suggest that the latter are stabilized by π -donor R' and σ - or π -bonded R groups. Calculations on the experimentally known complex Cl_3B-BCp^* suggest it is the strongest bonded donor-acceptor complex of main-group elements that has been synthesized until now. The electropositively substituted $Ge-AsX$ species are thermodynamically and kinetically more stable than their isomeric $XGe=As$ molecules according to B3LYP and CCSD(T) calculations⁴² for $X = H, Li, Na, BeH, MgH, BH_2, AlH_2, CH_3, SiH_3, NH_2, PH_2, OH, SH, F$ and Cl .

HF, MP2, CCSD(T) and B3LYP calculations⁴³ have been reported on the structures and bonding in mono $(CH)_5XH$ and disubstituted $(CH)_4(XH)_2$ substituted benzenes ($X = B^-, N^+, Al^-, Si, P^+, Ga^-, Ge$ and As^+). For the disubstituted isomers, the *ortho* isomer is more stable for $X = Ga^-, Ge$ and As^+ , the *meta* isomer is most stable for $X = B^-, N^+, Al^-$ and Si whereas the *para* isomer is most stable for $X = P^+$. B3LYP calculations⁴⁴ on the first stable germabenzene are in good agreement with its experimentally determined structure and properties whilst nucleus-independent chemical shift and aromatic stabilization energy calculations strongly indicate its aromaticity. B3LYP calculations⁴⁵ have been used to study the effect of substituents on the structure and bonding of polarized phosphalkenes revealing that the $P=C$ bond length is dependent on the π -back-donation of the substituent on P . Phosphole oligomers have interesting, tunable electronic properties due to competition between the cyclic- and the carbon backbone π -conjugation, according to HF and B3LYP calculations⁴⁶. Five and six membered cyclic carbenes containing phosphorus can be stabilized against dimerization by introduction of bridgehead tricoordinate phosphorus in the α -position from the carbene and/or tetracoordinate phosphorus in the β -position from the divalent carbon, according to B3LYP calculations⁴⁷.

The five-membered heterocyclic anion (*deloc*-1,3,4)-1-sila-3,4-diboracyclopentane-1-ide is strongly distorted at the MP2 level⁴⁸ and contains a three-centre-two-electron bond between silicon and two boron atoms. The difference in the C-C bond lengths in 1,2,4,5-tetrahydro-1,1,4,4-tetramethyl-1,4-disiladicyclobuta[*a,d*]benzene, the first silacyclobutene diannelated [*a,d*]benzene, results primarily from substituent effects and is not caused by ring strain effects, according to MP4 and B3LYP calculations⁴⁹.

The ionization potentials of the silenes ${}^iBuMe_2Si(Me_3Si)Si=Ad$ and $(Me_3Si)_2Si=Ad$ calculated⁵⁰ at the ROVGF, MP4/6, and B3LYP levels reproduce the experimental values and show that the effect of substituents on the HOMO energy of silenes is slightly smaller than in the corresponding alkenes.

The relative stabilities of the stereoisomers of the four-centre π systems $(\text{H}_2\text{X})\text{HE}=\text{EH}(\text{XH}_2)$, $(\text{H}_2\text{X})\text{HE}=\text{EH}(\text{XH}_2)^{2+}$, and $\text{HX}=\text{EHHE}=\text{XH}$ ($\text{E} = \text{Si}, \text{C}; \text{X} = \text{Al}, \text{B}, \text{P}, \text{N}$) correlate with by the orbital-phase continuity of the terminal atoms. Isodesmic reaction energies calculated at the MP2 and B3LYP levels⁵¹ show that π -conjugation is effective for stabilization of compounds with AlH_2 and BH_2 substituents on the unsaturated silicon, and therefore, aluminum- and boron-substituted disilenes can be potential synthetic targets. The structures and vibrational frequencies of $\text{Ga}(\mu\text{-H})_2\text{Ga}$ and $\text{In}(\mu\text{-H})_2\text{In}$, calculated at the BP86 level⁵², have enabled these matrix isolated species to be identified. MP2 and B3LYP studies⁵³ of Lewis base $\rightarrow \text{H}_2\text{Si}$ coordination shows that the strength of the interaction depends mainly on the nucleophilicity of the base and the extent of π -delocalization of the lone pair on the silylene onto the π -frame of the base and that the base coordination triggers the nucleophilicity of the silylenes. In contrast to earlier studies, the only silylene calculated to have a triplet ground state by a BLYP study⁵⁴ is bis(tri-*tert*-butylsilyl)silylene, $(t\text{-Bu}_3\text{Si})_2\text{Si}$.

23 minima on the potential energy surface of silabenzene have been identified using MP2, CCSD(T) and B3LYP calculations⁵⁵ including two new valence isomeric forms of silabenzene. 61 minima on the potential energy surface of disilabenzene, $\text{C}_4\text{Si}_2\text{H}_4$ have been identified using B3LYP and CCSD(T) calculations⁵⁶ with the planar forms corresponding to the most stable isomers but with several H-bridged isomers of high stability. 1-silanaphthalene is aromatic according to B3LYP calculations⁵⁷ of its structure, vibrational frequencies and NMR chemical shifts. The first stable 9-silaanthracene is similarly aromatic according to analysis of B3LYP calculations⁵⁸.

B3LYP calculations⁵⁹ on the structure of the overcrowded diaryldilithio-germane, $\text{Tbt}(\text{Dip})\text{GeLi}_2$ ($\text{Tbt} = 2,4,6\text{-tris}[\text{bis}(\text{trimethylsilyl})\text{methyl}]\text{phenyl}$; $\text{Dip} = 2,6\text{-diisopropylphenyl}$) confirm the structure determined experimentally. The monolithiated (organosulfonyl)acetonitriles $[\text{PhSO}_2\text{CHCNLi.TMEDA}]$ and $[\text{BuSO}_2\text{-CHCNLi.THF}]$ form novel chain and sheet polymeric structures in preference to the more common $(\text{SO}_2\text{Li})_2$ or Li_2N_2 ring dimers associated with lithiated sulfones or nitriles due to the inflexibility of the ligand backbone which precludes chelation and consequently destabilizing these structures, according to a B3LYP study⁶⁰. B3LYP calculations⁶¹ on the different isomers of 2,3-dihydro-1,2,4-thia-, seleno- and telluro-diphospholes, and 2,3-dihydro-1*H*-1,2,4-triphosphole indicate similar stability with the lone pair on the heteroatom able to conjugate with the adjacent double bond. B3LYP calculations⁶² on 8-X-1-(*p*- $\text{YC}_6\text{H}_4\text{Se}$) C_{10}H_6 , 8-G-C₁₀H₆SeH-1 and HG-SeH₂ ($\text{X} = \text{Cl}, \text{Br}, \text{and F}$) indicate that the conformation with the *p*- $\text{YC}_6\text{H}_4\text{Se}$ group perpendicular to the naphthyl group is most stable.

Orbital-phase theory⁶³ has been used to propose pentagon stability. Cyclic delocalization of the lone pair electrons on the five-membered ring atoms through the vicinal σ bonds was shown to be favoured by the orbital-phase properties. The pentagon stability was found to be outstanding in saturated phosphorus five-membered rings in the puckered conformation, and was substantiated by the negative strain energy of cyclopentaphosphane, P_5H_5 . The aromaticity of the all-metal molecules Al_4^{2-} , XAl_3 , Ga_4^{2-} , In_4^{2-} , Hg_4^{6-} , Al_3^- and

Ga_3^- aromatic units has been evaluated at the B3LYP level⁶⁴. All are electron deficient species compared to the corresponding aromatic hydrocarbons and all should be considered as having both π and σ -aromaticity. Cyclopropa-annulated benzenes, pyridines and phosphabenzenes are aromatic, cyclobutana-annulated analogues possess some aromaticity but cyclobutena-annulated analogues are not aromatic according to B3LYP calculations⁶⁵. The most stable isomer of Ge-containing cyanogens at the MP2, B3LYP and QCISD levels⁶⁶ is GeNCN resulting in the unpaired electron being localized on nitrogen.

2.2 Mechanistic Studies. – B3LYP and CAS- MCQDPT2 calculations⁶⁷ on the mechanism of the addition of nonenolizable aldehydes and ketones to $\text{Ge}=\text{C}$, $\text{Si}=\text{Si}$, $\text{Si}=\text{Ge}$, and $\text{Ge}=\text{Ge}$ bonds can be grouped as either involving the formation of singlet diradical or zwitterionic intermediates or as concerted processes. Reactions leading to Si-O bonds can proceed *via* diradical and zwitterionic intermediates but formation of a Ge-O bond does not proceed *via* diradical intermediates. The energy barriers for addition of water to nine silenes, studied at the MP4 and B3LYP levels⁶⁸, depend strongly on the substituents and show a good correlation with the difference in the total NBO charge between Si and C. B3LYP and QCISD calculations⁶⁹ on the abstraction reactions of silylenes with oxirane and thiirane show that the interactions involve the initial formation of a donor-acceptor ylide-like complex followed by a heteroatom shift *via* a two-center transition state. B3LYP and G2 studies^{70,71} of the MC_2H_6 ($\text{M} = \text{Si}$ and Ge) potential energy surface shows that MH_2 and C_2H_4 initially form a π -complex, which can either collapse to silirane (germirane) or can isomerise by a 1,2 H-shift to ethylsilylene (ethylgermylene) with a relatively low barrier.

The photoabsorption positions and symmetries for the discrete hole states in the dominant dissociation channel from photoionization of $\text{Ge}(\text{CH}_3)_4$ have been studied at the HF level⁷². The photodecomposition of $(\text{CH}_3)_3\text{SnI}$ has been investigated through CASSCF/MS-CASPT2 calculations⁷³ of the low-lying excited states and associated potential energy curves revealing that the a^1A' and b^1A' states are dissociative with respect to Sn-I bond elongation but that the upper c^1A' state is quasi-bound with respect to Sn-I bond elongation. The boron-zinc alkyl exchange reaction, studied at the B3PW91 level⁷⁴, is predicted to proceed with a low activation barrier, involving two intermediates with unusual bonding structures. The metal-carbon bonding in these intermediates ensures a highly stereoselective exchange process, which can be employed in asymmetric organometallic synthesis. 1,3-silyl migration on acylpolysilane proceeds *via* a retention pathway and an inversion pathway with respect to the stereochemistry of the migrating silyl group with the former energetically preferred, according to a B3LYP study⁷⁵. Silene undergoes $[2 + 2]$ cycloaddition with acetylene in a two-step manner resulting in the formation of silacyclobutene. The migration of silyl groups in silylpyrazolones proceeds *via* migration of the organosilyl group from the nitrogen atom to the oxygen atom (1,3-Si shift), followed by two consecutive 1,2-H shifts from the carbon to the nitrogen atom, according to a B3LYP and MP2 study⁷⁶.

The repulsive Coulomb barrier for several geometrically stable isomers of the

$[\text{BeC}_4]^{2-}$ dianion has been calculated at the HF level⁷⁷ with the electron-loss lifetime for the most stable linear isomer, $\text{C}_2^- \text{BeC}_2^-$, estimated to be about 5 ms. The potential energy surfaces for the reactions of atomic hydrogen with the methylgermanes, GeH_3CH_3 and $\text{GeH}_2(\text{CH}_3)_2$ have been studied at the PMP4SDTQ level⁷⁸ are in good agreement with available experimental values. The potential energy surface for the excitation of the $\text{Ba} \dots \text{FCH}_3$ complex to its electronic A' state, studied at the CASSCF and MRCI+Q levels⁷⁹, shows that the complex is repulsive at the ground state geometry and decays to Ba and CH_3F fragments. A MP2 study⁸⁰ of the reaction of atomic hydrogen with $\text{GeH}(\text{CH}_3)_3$ is in reasonable agreement with available experimental values within 298-510 K.

As an alternative to the standard Cossee mechanism, the dinuclear alternative of the olefin reactions at aluminium where the chain switches between two different metal centres at each insertion has been investigated at the B3LYP level⁸¹ which indicates that the barriers for both insertion and β -hydride transfer at two different metal centers are rather similar to those for the more usual mononuclear mechanisms. The formation of aromatic carboxylic acids by carboxylation of aromatics with a carbon dioxide- $\text{Al}_2\text{Cl}_6/\text{Al}$ system has been investigated at the B3LYP level⁸². A possible pathway involving an initial complex between benzene and Al_2Cl_6 , with subsequent formation of organoaluminum intermediates (PhAlCl_2 and PhAl_2Cl_3) is endothermic whereas the formation of $\{\text{AlCl}_3\}_n$ complexes of CO_2 is exothermic and presumably preferred.

The effect of geminal substitution at silicon on 1-sila- and 1,3-disilacyclobutane strain energies, 2+2 cycloreversion enthalpies and $\text{Si}=\text{C}$ π -bond energies have been studied using MP2 and MP4 calculations⁸³ on $\text{R}_2\text{Si}=\text{CH}_2$, 1-silacyclobutanes $\text{cyclo-R}_2\text{Si}(\text{CH}_2)_3$ and 1,3-disilacyclobutanes $\text{cyclo}(\text{R}_2\text{SiCH}_2)_2$. Electronegative substituents increase reaction enthalpies and strain energies and shorten and weaken the $\text{Si}=\text{C}$ π -bond. The transformation of 2,3-dimethyl-2-siloxy-1,1-disilyl-1-silacyclobut-3-ene to 1,2-dimethyl-3-(siloxydisilylsilyl) cycloprop-2-ene, studied at the B3LYP level⁸⁴, involves a typical 1,2-siloxy shift with a triangular geometry in the transition state, resulting in the formation of a cyclopropene ring. A B3LYP study⁸⁵ of the unimolecular rearrangement $\text{XSi}\equiv\text{P} \rightarrow \text{Si}=\text{PX}$ ($\text{X} = \text{H}, \text{Li}, \text{BeH}, \text{BH}_2, \text{CH}_3, \text{NH}_2, \text{OH}$ and F) suggests that highly electronegative substitution at silicon can greatly stabilize the triple-bonded $\text{XSi}\equiv\text{P}$ species relative to the double-bonded $\text{Si}=\text{PX}$ isomer, thermodynamically and kinetically. A similar study⁸⁶ of the unimolecular rearrangement of arsilyne, $\text{XSi}=\text{As}$ ($\text{X} = \text{H}, \text{Li}, \text{Na}, \text{BeH}, \text{MgH}, \text{BH}_2, \text{AlH}_2, \text{CH}_3, \text{SiH}_3, \text{NH}_2, \text{PH}_2, \text{OH}, \text{SH}, \text{F}$ and Cl), to arsilene, $\text{Si}=\text{AsX}$, also suggests that highly electronegative substitution occurs preferentially at silicon and, thus, strongly stabilizes triply bonded $\text{XSi}=\text{As}$, with respect to doubly bonded $\text{Si}=\text{AsX}$, again thermodynamically and kinetically. The delocalization energy in silanols, XH_2SiOH , and silanediols, $\text{XHSi}(\text{OH})_2$ ($\text{X} = \text{H}, \text{OH}, \text{OSiH}_3$ and Cl) increases on ionization with the $\text{Si}-\text{O}^-$ bond gaining a partial double bond character according to HF and B3LYP calculations⁸⁷.

A B3LYP study⁸⁸ reveals that *cis,trans*- $\text{Os}(\text{H})_2(\text{OTf})(\text{NO})(\text{P}^i\text{Pr}_3)_2$ and related systems react with $(\text{Me}_3\text{Si})_2\text{NLi}$, $(\text{Me}_3\text{Si})_2\text{CHLi}$, lithium 2,2,6,6-tetramethyl-

piperidine, $\text{Me}_3\text{SiCH}_2\text{Li}$, and $\text{B}(\text{CH}_2\text{SiMe}_3)_4^-$ by a highly unusual and facile $\beta\text{-Me}^-$ transfer with Me-C and Me-Si bond cleavage a direct $\text{S}_{\text{E}2}$ substitution at carbon with inversion of the Me group.

3 d- and f-Block Metals

3.1 Structural and Spectroscopic Studies. – 3.1.1 *Species Containing a Transition Metal-Carbon σ -Bond Including Metal-Carbonyls.* The electron density distribution in $[\text{FeCo}(\text{CO})_8]^-$, which contains a semi-bridging carbonyl has been determined through B3LYP / AIM calculations⁸⁹ to show the changes occurring during the evolution from terminal to bridging coordination. The smooth continuum of conformations observed in the solid state is explained in terms of the mutual interplay of direct M-M and M-CO and indirect M . . . M and M . . . C interactions. The vibrational frequencies of solvated $[\text{Ir}(\text{CO})_6]^{3+}$ calculated at the DFT level⁹⁰ have been used to assigned the experimental infrared spectrum and are consistent with the absence of IR \rightarrow CO π -back-bonding. BPW91 calculations⁹¹ on the vibrational frequencies of $[\text{CpFe}]_2(\mu\text{-CO})_2(\mu\text{-CH}_2)$ predict a $^3\text{B}_2$ ground state. The geometries, $\nu(\text{CO})$ frequencies, relative enthalpies and Gibbs energies of the alkene carbonyl complexes $[\text{W}(\text{CO})_4(\eta^2\text{-C}_2\text{H}_4)_2]^{0/+}$ and $[\text{W}(\text{CO})_5(\eta^2\text{-C}_2\text{H}_4)]$ have been studied at the B3LYP level⁹² and confirm experimental assignments.

The geometries, vibrational frequencies and bonding in OCAgX ($\text{X} = \text{F}, \text{Cl}, \text{Br}$) have been studied by *ab initio* calculations⁹³ revealing that the C-O distances are short, and the M-C distances are significantly longer than those in other molecules containing a metal-carbonyl bond. B3PW91 calculations⁹⁴ on $\nu(\text{CO})$ frequencies of the CO adducts of the bivalent lanthanides, $\text{Cp}_2\text{M}(\text{CO})_x$ ($\text{M} = \text{Eu}$ or Yb ; $x = 1, 2$, $\text{M} = \text{Ca}$; $x = 1$) are in good agreement with experiment for $\text{Cp}^*_2\text{M}(\text{CO})$ with $\text{M} = \text{Ca}, \text{Eu}$, but in poor agreement for $\text{M} = \text{Yb}$ unless the CO is bound to the metal through the oxygen atom. CASMCSF and MRSDCI calculations⁹⁵ have been used to study the bonding and structure of OUCO , $\text{O}_2\text{U}(\text{CO})_2$, and UO_2CO_3 and to assign the species present in matrices. A new conformer of $\text{Fe}(\text{CO})_4$ has been predicted using MP2 calculations⁹⁶ with a square planar configuration and a singlet ground state.

Computational and experimental studies⁹⁷ of the spectroscopy, photochemistry and electrochemistry of $[\text{M}(\text{CO})_4(\text{alpha-diimine})]$ complexes ($\text{M} = \text{Cr}, \text{Mo}$ and W) have been reviewed. B3LYP calculations⁹⁸ on the ground and excited states of $\text{fac-}[\text{Re}(\text{bpy})(\text{CO})_3(4\text{-Etpy})]^+$ provide assignments for the $\nu(\text{CO})$ modes in the MLCT excited state and show the importance of $\pi^*(4,4'\text{-X}_2)\text{bpy}^- \rightarrow \pi^*(\text{CO})$ mixing, providing an explanation for the relative intensities of the A_2' and A'' excited-state bands, and an explanation for the large excited-to-ground-state $\nu(\text{CO})$ shift for the A_2' mode and its relative insensitivity to variations in X. The halide ligands in $[(2,4'\text{-bpy})\text{RuCl}_2(\text{CO})_3]$ and $[(4,4'\text{-bpy})(\text{RuCl}_2(\text{CO})_3)_2]$ possess a significant role in the HOMO-LUMO energy gap and can be used to tune the electronic properties of ruthenium bipyridines, a B3PW91 study⁹⁹ suggests. A similar study¹⁰⁰ also suggests that the position of the bipyridine substituents in

mono(bipyridine) complexes of ruthenium (n,n' -L₂-2,2'-bpy)Ru(CO)₂Cl₂ ($n = 3, 4, 5, \text{ or } 6$; L = CO(O)Me or CO(O)Et) causes changes in their electrochemical properties of the compounds due to variations in the HOMO-LUMO energy gap.

Photolysis of Rh(CO)(PMe₃)₂Cl and Rh(CO)(PBu₃)₂Cl is predicted by B3LYP calculations¹⁰¹ to yield non-planar, spin-triplet, excited states whilst high energy photolysis of the former is predicted to yield *cis*-Rh(CO)(PMe₃)₂Cl. BPW91 calculations¹⁰² have been used to predict the products of the photolysis of (CpCo)₂FeSiH₂CH₃ and (CpCo)₂FeCH₂SiH₃. B3LYP calculations¹⁰³ of the linear and nonlinear ground state absorption in platinum-organic compounds show several ways to tailor the linear absorption to a desired wave length region with nonlinear absorption cross-sections strongly enhanced by the introduction of charge-transfer units and linear oscillator strengths essentially unaffected by the same ligand substitutions.

A DFT study¹⁰⁴ on Co(CO)₃(PPh₃)₂BEt₃ reveals that it contains a weak, novel B-O interaction. The EPR g-values for dinuclear radical anion complexes $\{(\eta\text{-L})[\text{Re}(\text{CO})_3\text{Cl}]_2\}^{\cdot-}$ (L = 2,2'-azobispyridine and 2,2'-azobis(5-chloropyrimidine)) are reproduced reasonably well by DFT calculations¹⁰⁵ which also provide insight into the relationship between spin density distribution and g-anisotropy. Molecular models for the reactivity of coordination vacancies of Ni-II ions grafted onto tridentate silica support with CO, studied at the B3LYP level¹⁰⁶, suggest that the Ni-CO interaction is stabilized by a magnetic transition from a Ni²⁺ triplet to the Ni²⁺ singlet state occurring upon adsorption. The photoelectron spectra of iron carbonyls have been modelled¹⁰⁷ showing that it is possible to track the temporal variation of a metal-carbon bond.

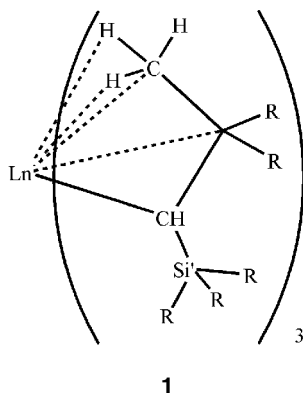
The structure and bonding in ruthenium porphyrin and carbonyl diyl complexes (CO)₄Ru-EH_{eq}, (CO)₄Ru-EH_{ax}, (Por)Ru-EH and (Por)Ru-E(trip) (trip – 2,4,6-triisopropylphenyl, E = B, Al, Ga, In, Tl) have been calculated at the B3LYP level¹⁰⁸. NBO analyses reveal high Ru-E bond dissociation energies, with B-Ru π -back-bonding similar to that in a M-CO bond. There is no correlation between the M-P bond lengths and bond strengths in the phosphines M(CO)₅PX₃ (M = Cr, Mo, W; X = H, Me, F, Cl), reveals a BP86 study¹⁰⁹, and PMe₃ forms the strongest and longest M-P bond whilst PCl₃ is the poorest σ -donor and a strongest π (P) acceptor. The π effects associated with Rh-P bond lengths, $\nu(\text{CO})$, and $-\Delta H_{\text{reaction}}$ for Rh(CO)(Cl)(PX₃)₂ and $\nu(\text{CO})$ and $-\Delta H_{\text{reaction}}$ for Rh(acac)(CO)(PZ₃) have been studied using a QALE analysis¹¹⁰ showing the importance of the synergistic interactions between the phosphine and other ancillary ligands.

The thermodynamics of H₂, arene, alkane, and CO addition to pincer-ligated three-coordinate d⁸, four-coordinate d⁸, and five-coordinate d⁶ iridium complexes, studied at the B3LYP level¹¹¹, suggest that addition of one ligand is favoured by π -donor ligands but addition of a second is disfavoured by such ligands. Protonation of [Re₂H(CO)₉]⁻ yields the neutral complex [Re₂H₂(CO)₉] which contains classically bonded, containing one μ_1 and one μ_2 H-atom but the non-classical [Re₂(η^2 -H₂)(CO)₉] tautomers is an intermediate in the fast hydride exchange process, according to B3LYP calculations¹¹². [W(N₂Npy)(NPh)Me]⁺

reacts with CO₂ or isocyanates *via* cycloaddition reactions at the W = NPh bond and not insertion into the W-Me bond, despite the latter product being the most thermodynamically favourable according to DFT calculations¹¹³. The d⁴ imido complex [TpRu(CO)(PPh₃)(NPh)][OTf] is thermally unstable due to the π -conflict arising from the π -antibonding role of the singly occupied molecular orbital, a B3LYP and BLYP study¹¹⁴ reveals.

BP86 calculations¹¹⁵ have been used to model the structures and NMR spectra of (L)PtMe_n (n = 2 or 4 and L = 1-methyl-(2-methylthiomethyl)-1*H*-benzimidazole and 1-methyl-(2-*tert*-butylthiomethyl)-1*H*-benzimidazole). The low-lying electronic transitions of a series of [ⁱPr-DAB)PtR₂] (R = CH₃, CD₃, adme, neop, neoSi, ^tBu, CPh, Ph, Mes) compounds have been studied¹¹⁶ at the DFT level revealing the significant R contribution to the high-lying orbitals and the MLCT with partial M-C σ -bond-to-ligand charge transfer character of the transitions. First row transition metals prefer N-binding while 2nd and 3rd row metals can prefer C-binding to imidazole according to DFT studies¹¹⁷. B3LYP calculations¹¹⁸ suggest that [Pd(COD)Cl] (L = 2,6-bis(diphenylphosphine sulfide)-3,5-diphenylphosphinine) contains a λ^4 -1-*P*-chlorophosphinine ligand, bound to the palladium atom through the phosphorus atom and is formed from the internal attack of the chloride counteranion onto the highly electrophilic P atom of the transient λ^3 -phosphinine complex. The structures of [Pd(μ -OAc)₂]₃, Pd(OAc)₂.2NHET₂, [Pd(OAc)(μ -OAc)(CH₃)₂SO]₂, [Pd(μ -OAc)(p-SEt)]₄ and [Pd(μ -SEt)₂]₆, calculated at the PBE level¹¹⁹, are in good agreement with X-ray diffraction analyses. The dicyanodicarbonyliron(II) thiolate complexes *trans*, *cis*-[(CN)₂(CO)₂Fe(S, S-C-R)]⁻ (R = OEt, NEt₂) are five-coordinate with a vacant site *trans* to the CO ligand and two CN- ligands occupying *cis* positions, according to B3LYP calculations¹²⁰. The coordination around the metal in [M(η^2 (C,C')-C₃O₂)(PPh₃)₂] (M = Ni, Pd, Pt) complexes is square planar according to BP86 calculations¹²¹. HF and MP2 calculations¹²² predict that relative energy of the isomers of *trans*-[PtCl₄{(*E*)-NH=C(Me)OEt}₂], *trans*-[PtCl₄{(*E*)-NH=C(Et)OEt}₂], *trans*-[PtCl₄{(*E*)-NH=C(Et)OⁿPr}₂], *trans*-[PtCl₄{(*E*)-NH=C(Et)OⁿPr'₂}, and *cis*-[PtCl₄{(*E*)-NH=C(Et)OMe}₂] decrease in the order *EE* > *EZ* > *ZZ*. The structures of (η^2 -fumarodinitrile) palladium(0) complexes containing dihydro(phosphanylphenyl)oxazole ligands are accurately reproduced by B3LYP calculations¹²³ but require extended basis sets on the metal.

The performance of DFT in studying¹²⁴ the structures of lanthanides organometallic complexes has been reviewed. The 4f electrons are shown to be uninvolved in bonding and can be included in the core but careful modelling of ligands is necessary as oversimplification can lead to structural artefacts. The peculiar pyramidal coordination observed experimentally for Ln[CH(SiR₂R')(SiR₃)₃] (Ln = La, Sm, R = R' = Me, R = H, R' = Me, R = R' = H) is reproduced by B3LYP calculations¹²⁵. The Si-C bond lengths are lengthened due to β -Si-C agostic interactions, whereas γ -C-H agostic interactions are repulsive, **1**.



HF calculations¹²⁶ confirm the experimental observation that the two N-N distances in $[\text{Rh}(\text{tpy})(\text{bpy})(\text{N}_3)](\text{PF}_6)_2$ differ. B3LYP calculations¹²⁷ on $[\text{Pt}(\text{COMe})\text{Cl}\{\text{MeN}(\text{H})\text{CH}=\text{CHN}(\text{Me})\text{C}(\text{O})\text{Me}\}]$ and the free ligand $\text{MeN}(\text{H})\text{CH}=\text{CHN}(\text{Me})\text{C}(\text{O})\text{Me}$ show that the internal H-bonding in the ligand is lost upon coordination. The W-W bond order in $[\text{W}_2(\kappa^2\text{-O}_2\text{CH})_4(\mu\text{-HCCH})_2]$, at the B3LYP level¹²⁸, is two. The intramolecular XH...HM interaction between the imine proton donor and the terminal hydride in $\text{H}(\mu\text{-H})\text{Os}_3(\text{CO})_{10}(\text{HN}=\text{CPh}_2)$ is essentially electrostatic, a B3LYP study reveals¹²⁹. The structures and frontier orbitals of $[\text{M}(\text{tmtaa})]$ and $[\text{M}(\text{acacen})]$ fragments employed in the organometallic chemistry of early transition metals have been investigated at the BP86 level¹³⁰. The Ir-I bond enthalpy in $[\text{Ir}(\mu\text{-S}^t\text{Bu})\text{I}_2(\text{CO})_2]_2$ is significant smaller than in $\text{trans-}[\text{Ir}(\text{X})\text{I}_2(\text{CO})(\text{PPh}_3)_2]$ ($\text{X} = \text{F}, \text{Cl}$ and Br) and is therefore, not transferable between both types of molecules, according to B3LYP calculations¹³¹, despite very similar bond lengths and bond orders. BP86 calculations¹³² on the structures and vibrational spectra of $\text{Re}(\text{CO})(\text{PMe}_3)_3(\eta^2\text{-BH}_4)$, $\text{Re}(\text{CO})(\text{PMe}_3)_3(\eta^2\text{-BBNH}_2)$, $\text{Re}(\text{CO})_2(\text{PMe}_3)_2(\eta^2\text{-BH}_4)$ and $\text{Re}(\text{CO})_2(\text{PMe}_3)_2(\eta^2\text{-BBNH}_2)$ have been used to confirm and assign the synthesis of these systems. BP86 calculations¹³³ have also been used to calculate the structure, relative energy, IR and ¹¹B NMR spectra of various isomers of $\text{Tp}^{3\text{R},5\text{R}}$ rhodium(I) dicarbonyl complexes (Tp = hydridotris(pyrazol-1-yl)borate; $\text{R} = \text{H}, \text{Me}$) revealing that the the lowest energy structure of $\text{Tp}^{3\text{R},5\text{R}}\text{Rh}(\text{CO})_2$ is a non-classical square pyramidal structure with a long metal apical ligand distance. B3LYP calculations¹³⁴ indicate a marked preference for homochiral dimeric fencholate methylzinc complexes over heterochiral dimers with H and Me ortho-substituents in the anisyl moieties but similar stabilities are predicted for SiMe_3 and ^tBu substituents.

B3LYP calculations¹³⁵ on $[\text{Os}_3(\mu\text{-H})(\text{CO})_{10}(\mu\text{-NC}_5\text{H}_3\text{C}_5\text{H}_4\text{N})]$, $[\text{Os}_3(\mu\text{-H})(\text{CO})_{10}(\mu\text{-NC}_5\text{H}_3\text{C}_5\text{H}_3\text{N})\text{Os}_3(\mu\text{-H})(\text{CO})_{10}]$ and $[\text{Os}_3(\mu\text{-H})(\text{CO})_{10}(\mu\text{-NC}_5\text{H}_3\text{C}_5\text{H}_4\text{N})\text{W}(\text{CO})_5]$ reveal that they all have similar orbitals in the LUMO region and that the first two have the Os---Os σ -bonding orbitals as their HOMO orbitals whilst the latter has the t_{2g} set orbitals of the $\text{W}(\text{CO})_5$ fragment as the HOMO orbitals. B3LYP calculations¹³⁶ suggest that the electronic coupling between the M_2 units in dimetal tetracarboxylates, $\text{M}_2(\text{O}_2\text{CR})_4$ ($\text{R} = \text{alkyl}$

and $M = Mo$ or W) occurs by $M_2 \delta \rightarrow$ ligand π -conjugation. B3LYP and BLYP calculations¹³⁷ on $Os_3H(\mu-H)(CO)_{10}(\text{benzylamine})$ show the presence of an unconventional hydrogen-bond $M\cdots H\cdots H\cdots N$. The structure of the first known triosmium carbonyl cluster with a coordinated redox-active ligand 4,4',5,5'-tetramethyl-2,2'-biphosphinine has been confirmed by B3LYP calculations¹³⁸ which also show that each P atom bridges two metal atoms.

A review of computational and crystallographic studies of the utility of Tolman cone for P-donor and other ligands in accounting quantitatively for steric effects has been published¹³⁹. Theoretical advances in the elucidation of the nature, the structure, the spectral and energetic characteristics of the new types of hydrogen bonds (HB) specifically for organometallic compounds – cationic hydride as a proton donor ($[MH](+) \dots OP(X-)$) and a metal atom ($M \dots HX$) or hydride ligand ($MH \dots HX$) as a proton acceptor – have been reviewed¹⁴⁰. The coordination and organometallic chemistry of metal-NO complexes¹⁴¹ and the interactions of organic nitroso compounds with metals¹⁴², including key computational and bonding studies, have been reviewed.

3.1.2 Cyclopentadienyl Derivatives and Related π -Bonded Species. The $Et_2C_2B_4H_4^{2-}$ carborane ligand in the ferrocenyl derivative ($\eta^6-C_6H_6$)Fe($Et_2C_2B_4H_3-5-Fc$) is strongly electron donating so that there is a substantial flow of electron density from the ferracarborane cluster to the ferrocenyl moiety, according to a PM3 and B3LYP study¹⁴³. A B3LYP and BP86 study¹⁴⁴ of the bonding in ferrocene derivatives with Group-15 heteroligands $Fe(\eta^5-E_5)_2$ and $FeCp(\eta^5-E_5)$ ($E = N, P, As, Sb$) reveals that the strongest bonded homoleptic complex is $Fe(\eta^5-P_5)_2$ and that the bonding in the mixed $FeCp(\eta^5-E_5)$ is much stronger than in the homoleptic molecules. The bonding in transition-metal boryl complexes of the type $[(C_5R_5)M(CO)_2BX_2]$ is dominated by the covalent contribution with σ -donation from the boryl ligand overwhelmingly predominating over π -back-donation, according to a B3LYP and BLYP study¹⁴⁵. $\eta^1-W(CO)_5$ and $\eta^5-M(CO)_3$ complexes ($M = Mo, W$) of 1,2,4- and 1,3,4-thiadiphospholes, $P_2SC_2Bu^t_2$, have similar stabilities, a B3LYP study reveals¹⁴⁶. Diphosphaferrocene bonds to $[GaCl_2]^+$ using the lone pairs on the phosphorus atoms with a contribution from the P-Fe bond, according to a BP86 study¹⁴⁷. The structures and energetics of $Au(C_5H_5N)^+$ species have been studied at the MP2 and CCSD(T) levels¹⁴⁸ revealing C_{2v} and C_1 symmetry isomers.

The Jahn-Teller distortion in $CrCp^*Tp$ has been studied using DFT calculations¹⁴⁹ and is due to the metal-based HOMO which is significantly antibonding with respect to a single pyrazolyl ring only. Both the singlet and triplet low-energy states of $[(\eta^6\text{-benzene})Nb(CO)_3]^+$ are subject to Jahn-Teller effects, according to a B3LYP study¹⁵⁰. The η^6, η^6 -inter-ring haptotropic rearrangement of (η^6 -biphenylene)chromium tricarbonyl has been studied at the PBE level¹⁵¹. B3LYP calculations¹⁵² have been reported on $(\eta^5-C_5H_5)Fe(CO)_2Cl$ and its fragments in anionic, neutral and cationic states and have been used to assign mass spectrometry experiments on anions.

A review of crystallographic and computational results and new BP86 and B3LYP calculations¹⁵³ show that the rotation angles in $MInd_2$ complexes show a

wide range of values, depending both on the electron count and on the steric effects of the ring substituents with hapticity change toward η^3 induced by extra electrons. The hapticity and ring slippage in $\text{IndMo}(\eta^3\text{-Ind})(\text{CO})_2$ has been investigated at the B3LYP level¹⁵⁴. Exocyclic η^3 coordination for the fluorenyl, cyclopenta[def]phenanthrenyl and dihydrocyclopenta[def]phenanthrenyl ligands in the complexes $\text{IndMo}(\text{L})(\text{CO})_2$ according to B3LYP calculations¹⁵⁵. The two-electron reduction driven η^5 to η^3 coordination shift of cyclopentadienyl and indenyl ligands in molybdenocene complexes, $[\text{X}(\eta^5\text{-Cp})\text{Mo}(\text{CO})_2]$ ($2+$) ($\text{X} = \text{Cp}$ or Ind) has been studied at the B3LYP level¹⁵⁶. The results verify the indenyl effect, that the rearrangement is much more facile for the indenyl ligand than for the cyclopentadienyl ligand, but suggest that this is due to the Mo-X bond strength rather than the traditionally accepted aromaticity gain in the benzene ring formed in $\eta^3\text{-Ind}$ complexes.

The energy profiles for the rotamers of mixed cobaltacarbonanes have been calculated at the ZINDO level¹⁵⁷. The photochemistry of the CpNiNO complex has been investigated¹⁵⁸ using DFT and time dependent DFT. The whole potential energy curve along the NiNO angle coordinate reveals both ground and metastable states, and transition states connecting the minima. The electronic influence of unbridged and ansa-bridged ring substituents on a zirconocene centre, studied at the BP86 level¹⁵⁹, suggest that the effects of substituents on the cyclopentadienyl rings are due to a simple inductive effects but that the electron-withdrawing effect of $[\text{Me}_2\text{C}]$ and $[\text{Me}_2\text{Si}]$ ansa-bridges is due to stabilization of the cyclopentadienyl ligand acceptor orbital, which enhances back-donation from the metal. BP86 calculations¹⁶⁰ of the structures and bonding in the complexes $\text{Cp}(\text{CO})_2\text{FeX}$ predict a widened angle at the carbon atom for $\text{X} = \text{CH}_2\text{SiH}_2(\text{OH})$ compared to $\text{X} = \text{CH}_3$, in agreement with the expectations of Bent's rule, and that X is weakly bound.

The bonding and structure of benzene complexes of V^+ , Cr^{2+} , Mn^+ , Fe^{2+} , Co^+ , Ni^{2+} and Cu^+ have been studied at the B3LYP level¹⁶¹ revealing large interaction energies. A B3LYP study¹⁶² predicts that benzene binds *via* its π electrons whereas pyridine forms σ complexes in the $[\text{Fe}(\text{L})(\text{L}')^n]^+$ ($\text{L}, \text{L}' = \text{benzene}$ or pyridine ; $n = 1$ or 2). There is a strong perturbation of the metal centres by the hydrazone bridge in $[\text{CpFe}(\eta^6\text{-p-HC}_6\text{H}_4\text{-NHN}=\text{CMe}-(\eta^5\text{-C}_5\text{H}_4)\text{FeCp})^+\text{PF}_6^-]$ as well as some metal-metal interaction through the bridge, a B3LYP study¹⁶³ reveals. A B3LYP study¹⁶⁴ confirms crystallographic results that the heterodimetallic complex $[\text{Zn}\{(\eta^5\text{-C}_5\text{H}_5)\text{Fe}[(\eta^5\text{-C}_5\text{H}_4)\text{-CH}=\text{N}-(\text{CH}_2)_3\text{-NMe}_2]\}\text{Cl}_2]$ exists in two isomeric forms which differ in the conformation of the ligand *E*(*anti*-) or *Z*(*syn*-). HF calculations¹⁶⁵ on $[\text{Nb}(\eta^5\text{-C}_5\text{H}_5)_2\text{PDT}]$ ($\text{PDT} = \text{propane-1,3-dithiolate}$), $[\text{NbCp}_2\text{EDT}]$ and $[\text{NbCp}_2\text{EDT}]^+$ ($\text{EDT} = \text{ethane-1,2-dithiolate}$) indicate a tetrahedral configuration around Nb, in agreement with crystallographic studies.

LDA and BP86 calculations¹⁶⁶ on the vibrational spectra of model complexes have been used to identify Zr-Cl, Zr-CH₃ and Zr-Cp bonds present in 2,2'-bis-(indene-2-yl)-biphenyl-Zirconium dichloride supported on silica in the presence of methylaluminumoxane. B3LYP, B3P86 and mPW1PW91 TDDFT calculations¹⁶⁷ have been used to study the UV/visible absorption spectra of rac-

Et(Ind)₂ZrCl₂, rac-Et(Ind)₂ZrMeCl, rac-Et(Ind)₂ZrMe₂, and the [rac-Et(Ind)₂ZrMe-C₂H₄]⁺ complex and reproduce fairly well the essential features of the experimental spectra which originate from ligand to metal charge transfer transitions. DFT calculations¹⁶⁸ confirm the X-ray structure of {[Cp-C(=CH₂)-O]-Zr(NEt₂)₂}₂ with the two Zr centres connected by two symmetry-equivalent η⁵:κ[Cp-C(=CH₂)-O] ligands.

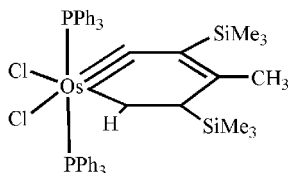
B3PW91 calculations¹⁶⁹ have been used, in conjunction with an electron diffraction study, to study the structure of Ru(C₅Me₅)(C₅F₅), Ru(C₅H₅)₂, Ru(C₅F₅)(C₅H₅) and Ru(C₅F₅)₂, revealing that F substituents, while σ-electron withdrawing in nature, donate to the ring π-systems resulting in shorter ruthenium-to-ring distances. B3LYP calculations¹⁷⁰ on ferrocenophanes yield structures in good agreement with those determined experimentally. BP86 calculations¹⁷¹ have been used to rationalize the bonding in [Rh₂(μ-O₂CR)₄L] complexes with strong and very weak axial donor-acceptor ligands L such as ‘Arduengo’ carbenes and aromatic hydrocarbons.

The structures and vibrational frequencies of Tp(3,5-Me)RhH₂(H₂) in its ground and various transition states have been studied at the B3LYP and BP86 levels¹⁷² revealing canted η²-dihydrogen dihydride local minima. The diabatic couplings between the metal centre in [MCp₂]^{0/+} (M = Fe, Co; Cp = C₅H₅) have been evaluated¹⁷³ using *ab initio* methods at the HF level leading to excellent agreement with the experimental estimate for M = Fe. For M = Co, the calculated numbers are substantially higher than the experimental estimates, suggesting that the latter may represent a considerable underestimate. The dissociation of the (C₆H₆)Cr(CO)₃⁺ ion proceeds by the sequential loss of three CO and benzene ligands, according to BP86 calculations¹⁷⁴. DFT calculations¹⁷⁵ of the electronic structure and normal vibrational modes of CpRe(NO)(CO)H support the localized two-electron valence bond description of the Re-H interaction suggested by the vibrational progressions seen in the valence ionization spectrum. Calculated H-D and H-T coupling¹⁷⁶ in [Cp/Cp*Ru(P-P)H₂]⁺ (where P-P is a chelating diphosphine ligand) are consistent with experimental studies of their dependence on temperature and magnetic field.

The molecular structures and excited states of CpM(CO)₂ (M = Rh, Ir) and [Cl₂Rh(CO)₂]⁻ have been investigated at the B3LYP and SAC-Cl levels¹⁷⁷ suggesting that they have singlet ground electronic states with large singlet-triplet separations. The strong transitions in [Cl₂Rh(CO)₂]⁻ are identified to be metal to ligand CO MLCT excitations but in the CpM(CO)₂ systems both MLCT excitation and ligand Cp to metal and CO charge transfer excitation are strongly mixed. The unsaturated metal centre in (phenylbicycloheptenyl)Pd(PPh₃) and related substituted derivatives receives π-electron density of the arene mainly through its C-*ipso* atom and this effect may be slightly improved if the C-*ortho* atom also gets closer to the metal but the slipped η² coordination does not appear seem to be crucial for the stability of the system according to B3LYP calculations¹⁷⁸. B3LYP calculations¹⁷⁹ suggest that the six membered metallacycle in osmabenzynes Os[≡C-C(SiMe₃)=C(CH₃)-C(SiMe₃)=CH]Cl₂(PPh₃)₂ exhibits somewhat aromatic properties with the filled metal d_{x²-y²}-orbital interacting with the equatorial p-orbital of the high

reactive carbyne carbon in a back-bonding fashion.

BP86 calculated¹⁸⁰ dipole moments of $(\eta^5\text{-C}_5\text{H}_5)(\text{PH}_3)_2\text{M}(\text{C}\equiv\text{C-}p\text{-C}_6\text{H}_4\text{X})^{n+}$ ($\text{M} = \text{Fe, Ru}$; $\text{X} = \text{NO}_2, \text{CN, H, OMe, NH}_2$; $n = 0, 1$) have been used to calculate second-order molecular polarizabilities with electron-rich iron sigma-aryl acetylide.



2

A molecular mechanics force field has been developed¹⁸¹ for the conformational analysis of amido- and alpha-aminoferrocenes and used to show that the selectivity of the diastereoselective lithiation of N,N-dimethylferrocenylethylamine and sparteine-mediated enantioselective lithiation of (diisopropylamido)ferrocene using MeLi from the adduct conformer with the shortest C-H-ring---H₃C-Li interaction. The 16e two-legged piano-stool complexes $[\text{CpRu}(\text{PP})]^+$ ($\text{PP} = (\text{PH}_3)_2, \text{H}_2\text{PCH}_2\text{CH}_2\text{PH}_2$) adopt typically pyramidal structures whereas $[\text{CpRu}(\text{NN})]^+$ ($\text{NN} = (\text{NH}_3)_2, \text{H}_2\text{NCH}_2\text{CH}_2\text{NH}_2$) prefer planar structures, according to B3LYP calculations¹⁸².

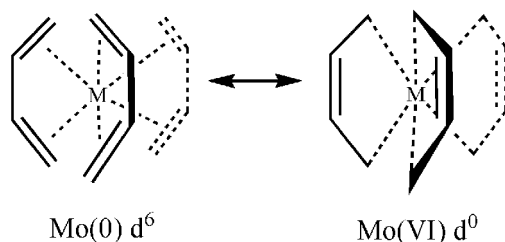
A combined molecular mechanics, PM3 and BOP study¹⁸³ of binding of $\text{CH}_2=\text{CHR}$ to chiral $[(\eta^5\text{-C}_5\text{H}_5)\text{Re}(\text{NO})(\text{PPh}_3)]^+$ ($\text{R} = \text{Me, } n\text{-Pr, CH}_2\text{Ph, Ph, } ^i\text{Pr, } ^t\text{Bu and SiMe}_3$) has been used to study the stereoselectivity allowing computationally derived diastereoselective excess to be derived and compared with experiment. The Cr-C₂X₄ bond strengths in $\text{Cr}(\text{CO})_5(\text{C}_2\text{X}_4)$ ($\text{X} = \text{H, F, Cl}$) has been investigated using a DFT and bond energy decomposition analysis¹⁸⁴ in terms of the Dewar-Chatt-Duncanson model suggesting that the energy necessary to deform the olefin and the metal-centered fragment is the determining factor in the trends in bond enthalpies. A B3LYP study¹⁸⁵ has shown that styrene oxidation by chromylchloride yields an intermediate with a 2:1 stoichiometry with two Cr(V) centres on opposite sides of the former double bond.

A B3LYP study¹⁸⁶ suggests that back-donation is important for olefins but electron donation is more important for phosphanes in $[\text{Pt}(\text{PH}_3)_2\text{L}]$ ($\text{L} = \text{H}_2\text{C}=\text{CHR}$ or PH_2R , $\text{R} = \text{H, CN, F, OH, NH}_2$) complexes. Complexation of azaphosphirane with $\text{W}(\text{CO})_5$ is predicted by B3LYP calculations¹⁸⁷ to lead to a tighter ring. BP86 and B3LYP calculations¹⁸⁸ on $[\text{Nb}(\eta^5\text{-C}_5\text{H}_5)\text{R}_2(\text{HCCH})]$ ($\text{R} = \text{Cl, Me}$) have been used to study the parallel and the perpendicular conformations of the alkyne ligand with respect to the Cp plane and suggest that the latter is preferred. The Os-C(alkyne) distance shortens between the complex $\text{Os}(\eta^5\text{-C}_5\text{H}_5)\text{Cl}\{\eta^2\text{-HC}\equiv\text{CC}(\text{OH})\text{Ph}_2\}(\text{P}^i\text{Pr}_3)$ $[\text{Os}(\eta^5\text{-C}_5\text{H}_5)\{\eta^2\text{-HC}\equiv\text{CC}(\text{OH})\text{Ph}_2\}(\text{P}^i\text{Pr}_3)]\text{PF}_6$ due the participation of the acetylenic second π -orbital in the metal-alkyne bonding so that the 2-electron-donor alkyne ligand transforms to a 4-electron-donor ligand, a B3LYP study reveals¹⁸⁹. The structures of [1,2-

$(\text{CH}_2)_2\text{C}_5\text{Me}_3\text{MC}_5\text{Me}_4\text{CH}_2]^{3+}$ trications ($\text{M} = \text{Ru}$ and Os) have been calculated at the BLYP level¹⁹⁰. The Pt-Ga bond length in $\{(\text{dcpe})\text{Pt}[\text{GaC}(\text{SiH}_3)_3]_2\}$ is very short, a BP86 study reveals¹⁹¹, with significant Pt→Ga π -back-donation.

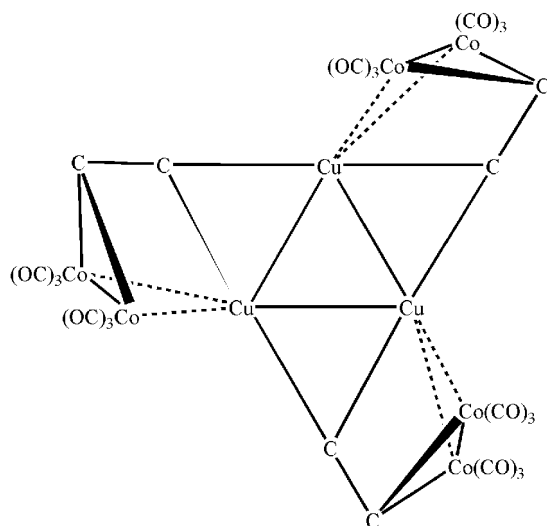
The trans and cis isomers of $[\text{PdCl}_2(\text{L-Allyl})_2]$ ($\text{L-Allyl} = 1,3$ -diallylimidazolidin-2-ylidene) have comparable stability, according to a B3LYP study¹⁹². The barrier to alkyne rotation in $[\text{H}_3(\text{CO})(\text{I})\text{W}\{\text{HC}\equiv\text{CH}\}]^{2-}$ and $[\text{H}_3(\text{CO})(\text{I})\text{W}\{\text{HC}\equiv\text{CCH}_2\}]^{3-}$ is calculated, at the extended Hückel level¹⁹³, to be too high for rotation to be important on the NMR timescale. A BP86 study¹⁹⁴ has shown that the ^1H NMR spectrum of paramagnetic $(2\text{-Me-allyl})_3\text{Cr}$ can be explained by the presence of two conformers which convert into each other by rotation of one allyl ligand around the allyl-chromium axis.

The unusual trigonal prismatic structure of tris(butadiene)molybdenum **3** has been confirmed by calculations at the MP2, BP86 and B3LYP levels¹⁹⁵. NBO and NRT analyses of the bonding suggest coordination of diolefins to a d^6 Mo(0) atom is a more accurate description than M-C σ -bonding of a olefin to d^0 Mo(VI). The bonding in the unusual $\text{Cu}_3\{\mu^2\text{-(CCHCO}_2(\text{CO})_6\}_3$ cluster **4** has been studied using a DFT calculations¹⁹⁶ to provide a rationalization of its peculiar structure, suggesting that the triangular Cu(I) core interacts strongly with the organometallic fragment with an important π component. The bonding in the 46-electron cluster $[(\text{CO})_3\text{Fe}(\mu_3\text{-Se})\{\text{Pt}(\text{CO})\text{P}(2\text{-C}_3\text{H}_4\text{N})\text{Ph}_2\}_2]$ consists of an open Pt---Fe---Pt triangle capped by a μ_3 -Se atom and can be thought of as a tetrahedral $(\text{CO})_3\text{FeSe}$ unit stabilized by sidewise interactions of the triple bond with two d^{10} - L_2M fragments, a B3LYP study¹⁹⁷ reveals. The chemical shift and electric field gradient tensors in the piano-stool compound mesitylenetricarbonylmolybdenum(0) have been calculated at the BP86-ZORA level¹⁹⁸ and are found to reproduce the experimental results.



3

The structures and bonding of the closo- $[1\text{-M}(\text{CO})_3(\mu^4\text{-E}_9)]^{4-}$ ($\text{E} = \text{Sn}, \text{Pb}; \text{M} = \text{Mo}, \text{W}$) cluster anions have been studied at the DFT level²¹. The bis(ferrocenyl)butadiyne ligand in $\text{Os}_3(\text{CO})_{10}(\mu_3\text{-}\eta^2\text{-FcC}_4\text{Fc})$ has triene character that facilitates electrocommunication through the unsaturated carbon chain, a molecular orbital analysis based on extended Hückel calculation has revealed¹⁹⁹. A B3LYP study²⁰⁰ reveals that the phosphalkyne ligand in $[\text{CpMo}\{\text{P}(\text{OH})_3\}_2\{\eta^2(4e)\text{-PC}\equiv\text{Me}\}]^+$ is a poorer donor and better acceptor than the alkyne ligand in $[\text{CpMo}\{\text{P}(\text{OMe})_3\}_2\{\eta^2(4e)\text{-alkyne}\}]^+$. Donor-acceptor interactions, studied at the B3LYP level²⁰¹, of Lewis bases, such as amine, phosphine, cyanic acid and phosphalkyne with various phosphinidene complexes



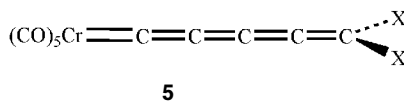
4

carrying a $W(CO)_5$ fragment can be divided into two categories. Amines bind stronger than a phosphine to a phosphinidene. π -donors yield shorter N-P bond, but the resulting donor-adduct is even less stable with respect to decomposition.

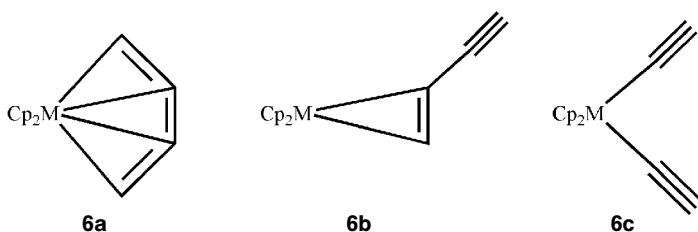
A B3LYP study²⁰² reveals that the greatest bonding contribution in the vinyl coordination to the $M(CO)_5$ fragment in $[M(CO)_5\{-\eta^2\text{-Ph}_3\text{PAuC(OR)=CH}_2\}]$ [$M = \text{Cr, R = Me, Et; M = Mo, R = Me; M = W, R = Me, Et}$] complexes comes from the terminal, partially negatively charged, CH_2 carbon atom *via* partial end-on η^1 -bonding rather than the usual η^2 -bonding of olefins. The Arduengo carbene ligand in a methyltitanocene cation complex serves as a pure σ -donor ligand to the titanocene moiety and the observed favoured 'in-plane' orientation of the ligand is steric in origin, according to a BP86 and bond energy analysis²⁰³.

The metal-cumulene bond in the series of metallacumulene complexes $[(CO)_5Cr(=C)_nX_2]$ ($X = \text{F, SiH}_3, \text{CHCH}_2, \text{NH}_2, \text{NO}_2; n = 2\text{-}8$) **5** are significantly affected by the substituents, particularly by the resonance effect in the NH_2 and NO_2 systems. A BP86 and bond energy analysis²⁰⁴ reveals that π -donor amino substituents cause a decrease in the bond strength while the π -acceptor nitro substituents cause an increase of the bonding energies, particularly for cumulenes with an odd or an even number of carbon atoms, respectively.

The conformations of complexes such as $[M_2(\mu\text{-C}\equiv\text{CR})_2L_4]$, in which each metal atom is in a square-planar environment depend on the coordination mode of the alkynyl ligands and the angle between the coordination planes around the two metal atoms, a MP2 study reveals²⁰⁵. Each metal centre in $[\text{Sm}(\text{NHAr})_3]_2$ engages in an η^6 -arene interaction with the aryl ring of an amide ligand attached to an adjacent samarium with a significant role for the 5d metal acceptor orbitals in stabilizing π -donation from the imido groups to the Sm centres within the Sm_2N_2 core, according to a B3LYP study²⁰⁶.



The relative energies of the isomers of C_5H_4 -cyclocumulene, ethynylcyclopropene, diethynylmethane, and their organometallic analogues obtained by replacing the CH_2 groups by Cp_2Ti and Cp_2Zr are dramatically altered in the transition-metal analogues according to a B3LYP study²⁰⁷. The metallacyclocumulenes **6a** are comparable in energy to **6c** and **6d** and substituents on the carbon skeleton help to fine-tune the energetics. The influence of the η^1 - and η^5 -pyrrolyl coordination modes on the stabilities of $[\text{pyr}^{\text{Ar}2}]\text{Zr}(\text{NMe}_2)_3$ and $[\text{pyr}^{\text{Ar}2}]\text{Zr}(\text{NMe}_2)_2$ ($\text{Ar} = \text{Ph}, \text{Xyl}$) has been examined at the B3LYP level²⁰⁸ suggesting that η^5 -coordination is favoured to a greater degree for the smaller $[\text{pyr}^{\text{Ph}2}]$ ligand than for the $[\text{pyr}^{\text{Xyl}2}]$ ligand, largely due to the increased bulk in the ortho positions destabilizing η^5 -coordination for the $[\text{pyr}^{\text{Xyl}2}]$ ligand.



A BP86 study²⁰⁹ suggests that the bonding of the ene-diamido ligand is different with respect to the conventional σ^2, π -description of the bonding of the *cis*-1,3-butadiene ligand to early transition metals. The experimentally observed folded envelope geometry in high valent early transition complexes containing a substituted 1,4-diaza-1,3-butadiene ligand is due to the reorientation of the N hybrid orbitals in order to saturate the metal centre. The valence structure for the $[\text{M} \cdots \text{C}_x \cdots \text{M}']$ unit in a variety of homonuclear $[\{\text{Cp}(\text{CO})_2\text{M}\}_2(\mu\text{-C}_x)]$ ($\text{M} = \text{Cr}, \text{Fe}^+, x = 3, 5, 7$) and heteronuclear $[\{\text{Cp}(\text{CO})_2\text{M}\}(\mu\text{-C}_x)\{\text{Cp}(\text{CO})_2\text{M}'\}]$ ($\text{M} = \text{Fe}^+, \text{M}' = \text{Mn}, x = 3, 5, 7$) model compounds is diagnostic of the metal-to-metal communication and a BP86 study²¹⁰ reveals a simple electron-counting scheme to predict the valence structure, based on the d^n configuration of the ML_m ($\text{M}'\text{L}'_m$) fragments and the number of p_π electrons of the 'linear' C_x unit. *trans*- $[\text{RhX}(\text{L})(\text{PMe}_3)_2]$ ($\text{L} = \text{C}=\text{CH}_2, \text{C}=\text{CHC}_6\text{H}_5, \text{CO}, 2,6\text{-Me}_2\text{C}_6\text{H}_3\text{NC}, \text{C}_2\text{H}_4$) complexes have been used as model compounds for the analysis of the vibrational spectra of related complexes at the BPW91 level²¹¹ allowing the *trans* influence of a series of ligands on the metal-carbon bond in vinylidene, carbonyl and isocyanide complexes to be studied. A molecular mechanics study²¹² of optically active ferrocene containing macrocyclic peptides reveals that the low energy conformations are non-symmetric. C-H... π interactions where the C-H group interacts with the π -system of a six-membered chelate ring take place in quite a number of metal complexes, including organometallic compounds and have bond energies of *ca.* 1 kcal mol⁻¹ at the B3LYP level²¹³.

3.2 Mechanistic Studies. – Chiral catalysts that are efficient at inducing asymmetry have their region of maximum stereinduction spatially congruent with the site of chemistry but inefficient catalysts do not according to study²¹⁴ of a range of catalysts for three Diels-Alder reactions at the PM3 and MM level. Theoretical and experimental studies of photochemical Pt-C bond homolysis reactions of metal-carbon bonded platinum compounds have been reviewed²¹⁵. The use of computational quantum chemistry in catalysis research has been assessed²¹⁶ suggesting that single reference theories are not sufficiently accurate and that a multi-configurational self-consistent field (MCSCF) theory must be utilized.

3.2.1 Polymerization Reactions. According to BP86 calculations²¹⁷ for a model system with $L = HC(O)CHC(O)H$, cationic titanium complexes of the type L_2TiR^+ ($R =$ growing alkyl chain) can be viable intermediates in the homogeneous olefin polymerisation catalysed by titanium beta-diketonato complexes. The interaction between the catalyst systems $(NPR_3)_2TiMe^+$, $(Cp)(NCR_2)TiMe^+$, $(CpSiR_2NR')TiMe^+$, $(Cp)OSiR_3TiMe^+$, and $(Cp)NPR_3TiMe^+$ and the counterions $B(C_6F_5)_4^-$, $MeB(C_6F_5)_3^-$, TMA-MAOMe⁻ and MAOMe⁻ (TMA = trimethylaluminum and MAO = methylalumoxane) have been studied at the BPW91 level²¹⁸. The ion-pair separation energies increase in the order $B(C_6F_5)_4^- < MeB(C_6F_5)_3^- < TMA-MAOMe^- < MAOMe^-$. For each counterion, the $(NPR_3)_2TiMe^+$ system has the lowest separation energy. QM/MM models satisfactorily reproduce the behaviour of the ion-pair system in the insertion process. Possible structural candidates for the active(III) and dormant (IV) species in dimethylzirconocene-catalysed, MAO (methylaluminoxane)-activated olefin polymerization have been identified at the BP86 level²¹⁹ as $[Cp_2ZrMeAlMe_3]^+ [MeMAO]^-$ (III) and $[Cp_2ZrMe]^+ [MeMAO]^-$ (IV) respectively.

A change in the olefin pressure does not affect the global number of branches in propylene polymerization catalysed by Pd(II) complexes with methyl backbone- and -Ph⁻Pr₂ imine substituents but strongly affects the polymer microstructure, leading to hyperbranched structures at low pressures, according to stochastic simulations using DFT energies²²⁰. The performance of DFT and *ab initio* approaches²²¹ in studying the propagation and termination reactions of olefins with a prototype homogeneous Group 4 *ansa*-metallocene catalyst has been compared leading to substantially similar geometries at all levels. Pure functionals underestimate the difference between termination and propagation but hybrid functionals lead to very similar energetics to CCSD(T). A reasonably good correlation has been observed at the B3LYP level²²² between the turnover frequency of Ni(II) salicylaldiminato catalysis for ethylene polymerization in the presence of additives and the Ni-O (additive) bond dissociation energy.

The unusual inverse kinetic isotope effect observed for the catalyst $[C_5Me_5(P(OCH_3)_3)CoCH_2CH_2-\mu-H]^+$ in the polymerization of ethylene is reproduced by a B3LYP study²²³ of the catalytic cycle. A B3LYP study reveals²²⁴ that ethylene is easily inserted into the Ni(II)-CH₃ bond of $Ni(CH_3)L]^+$ with a moderate activation barrier with $L = HNCH=CHNH$, $PhNCH=CHNPh$,

$\text{H}_2\text{PCH}_2\text{CH}_2\text{PH}_2$, and $\text{Me}_2\text{PCH}_2\text{CH}_2\text{PMe}_2$ but with a larger activation barrier with $\text{L} = 2,2'$ -bipyridine as the coordinate bond of the latter is less flexible. Coordination of ethylene with the nickel(II) propyl complex $[\text{Ni}(\text{CH}_2\text{CH}_2\text{CH}_3)\text{L}]^+$ involves a β -H agostic interaction which is weakest for $\text{L} = \text{Me}_2\text{PCH}_2\text{CH}_2\text{PMe}_2$ so allowing this system to propagate the reaction through coordination of further ethylene. A B3LYP study²²⁵ of the reaction of alkynes with $[\text{RuCp}(\text{PR}_3)(\text{CH}_3\text{CN})_2]\text{PF}_6$ ($\text{R} = \text{Me}, \text{Ph}, \text{Cy}$) leading to allyl carbene or butadienyl carbene complexes suggests that metallacyclopentatriene and vinylidene complexes, respectively, are crucial intermediates.

The effects of Me, ¹Bu, OMe, and F substitutions on the insertion aptitude and regioselectivity of propene with a cationic phenylpalladium(II)diimine catalyst have been studied at the B3LYP level²²⁶. There is a correlation for symmetrical substitutions between the stability of the catalyst HOMO and the insertion barrier whilst for unsymmetrical substitutions of F and OMe, trans-influences led to relatively large differences in insertion aptitudes. Steric effects are notable when ¹Bu replaced hydrogen at the nitrogen positions, primarily through the interaction between t-Bu and alkene methyl groups. The asymmetric induction observed in palladium-catalysed allylic alkylation reactions with typical substrates has been investigated at the BP86 level²²⁷ using three structurally related chiral PN ligands. The stereochemical outcome is determined by a delicate balance of steric repulsions and not by electronic effects.

The polymerization of ethene and propene by a dicyclopentadienyl yttrium hydride catalyst involves the overall reactions $\text{Cp}_2\text{YH} + 2\text{C}_2\text{H}_4 \rightarrow \text{Cp}_2\text{Y-C}_4\text{H}_9$, and $\text{Cp}_2\text{YH} + 2\text{C}_3\text{H}_6 \rightarrow \text{Cp}_2\text{Y-C}_6\text{H}_{13}$, and proceeds *via* formation of a weakly bound encounter complex between the monomer-catalyst and the olefin, followed by the insertion of the ethene or propene into a Y-C bond and finally the formation of a $\text{Cp}_2\text{Y-C}_4\text{H}_9$ or $\text{Cp}_2\text{Y-C}_6\text{H}_{13}$ species, according to a B3LYP study²²⁸. The semi-empirical PM3 method²²⁹ has been used to study the transition state of the olefin insertion process of metallocene catalysts leads to results which are in good agreement with those obtained at higher levels of theory. The mechanism of the enantioselective alkylation of aldehydes with diethylzinc using has been studied at the B3LYP level²³⁰. The mechanism of copolymerization of CO_2 with cyclohexene oxide catalysed by the Zn(II) organometallic compound (BDI)ZnOCH₃ has been studied using the ONIOM approach²³¹. Insertion of CO_2 into either a zinc-alkoxyl or zinc-carbonate bond is thermodynamically less favourable but kinetically favoured over the insertion of epoxide, due to a high barrier for the latter. The high barrier is associated with a rather asynchronous transition state where the ring opening has taken place and yet the C-O bond is not formed.

The nature of the monomer insertion step in the allylnickel(II)-catalysed 1,4-polymerization of 1,3-butadiene has been investigated in a BP86 study²³². Polymerization by the *trans*-1,4 regulating cationic allylnickel(II) $[\text{RC}_3\text{H}_4\text{Ni}(\text{C}_4\text{H}_6)\text{L}]^+$ catalyst proceeds *via cis*-butadiene insertion into either the η^1 - σ -butenyl-Ni bond or the η^3 - π -butenyl-Ni bond and anti-syn isomerization. B3LYP calculations²³³ on $[\text{Cr}(\text{NR})_2\text{C}_3\text{H}_7(\text{C}_2\text{H}_4)]^+$ ($\text{R} = \text{H}, ^1\text{Bu}$) reveal a facile reductive elimination reaction involving β -hydrogen transfer from the alkyl chain, suggesting

that the active species in ethylene polymerisation with bis(imido)chromium(VI) precursors contains a reduced chromium atom.

3.2.2 C-X Activation Reactions. The reaction pathways for the reactions of Ni and CH₄ leading to NiCH₂ + H₂, NiCH₃ + H and NiH + CH₃ have been studied at the B3LYP level²³⁴. Reaction of platinum oxide with methane at elevated temperatures leads to direct abstraction of a hydrogen atom leading to PtOH and free methyl radical, reveals a B3LYP study²³⁵. B3LYP studies²³⁶ on palladium and platinum alkoxide complexes containing bidentate ligands, L₂MX(OCY₂H) (L₂ = CH₂NCHCHNCH₂ and PH₂CH₂CH₂PH; M = Pd and Pt; Y = H and F) show that Pd complexes with X = OCH₃, NH₂, OH and HCOO favour σ -bond metathesis followed by a reductive elimination leading to the metal-hydride products while complexes with X = CH₃ favour β -hydrogen elimination. Both reaction pathways are possible for complexes with ligands X = Cl and Br when M = Pd and Y = H. Pt complexes have higher reaction barriers. B3LYP studies²³⁷ of palladium insertion into alkyne and aryl carbon-halogen bonds suggest that it can proceed *via* a concerted oxidative addition across the carbon-halogen bond. A stepwise mechanism *via* a σ -complex is favoured when a nitro group is introduced onto the alkyne.

The C-H bond dissociation reactions of methane and ethane by the bare FeO⁺ complex and diiron and dicopper models of methane monooxygenase, studied at the B3LYP level²³⁸, can proceed *via* pathways: oxene insertion in which a C-H bond is dissociated and C-O and O-H bonds are formed in a concerted manner *via* a three-centred transition state (CHO)-H-...-O-...-Fe, direct abstraction mechanism in which a linear transition state (CHO)-H-...-O-...-Fe leads to the dissociation into an Fe-OH intermediate and an alkyl radical species and a four-centred transition state (CHO)-H-...-O-...-Fe in its initial stages which leads to a reaction intermediate involving OH and CH₃ ligands. The parallel and perpendicular approach of the incoming substrate in the activation mechanism of the C-X (X = Sn, Ge, Si, C, H) σ -bonds of HC \equiv CR (R = SnH₃, GeH₃, SiH₃, CH₃, H) has been examined at the B3LYP level²³⁹ using the model complexes (PH₃)₂M (M = Ni, Pd, Pt). For X = Ge, Si, C, H, the C-X σ -bonds approach the Pd parallel to the P-Pd-P plane and are activated in the P-Pd-P plane. In contrast, the highly polarized C-Sn σ -bond, the C-Sn σ -bond approaches the Pd perpendicularly to the P-Pd-P plane. The reactions of Ti⁺(⁴F, ²F), V⁺(⁵D, ³F), and Cr⁺(⁶S, ⁴D) with NH₃ and CH₄, studied using DFT²⁴⁰, proceed *via* formation of the high-spin ion-dipole complex, followed by a hydrogen shift process leading to the formation of the insertion products, which are more stable in a low-spin state. B3PW91 calculations²⁴¹ of the potential energy and free energy of the C-F cleavage reaction of OsH₃ClL₂ (L = PPr₃) with vinyl fluoride to produce OsHFCl(=CCH₃)L₂ and H₂ proceeds *via* OsHCl(H₂)(H₂C=CHF)L₂. The unimolecular C-F cleavage of the coordinated C₂H₅F has a high activation energy. The dehydrogenation reaction of [μ^3 -2,6-(R₂PCH₂)₂C₆H₃]₃IrH₂ ‘pincer’ complexes may proceed *via* classical Ir(V) and nonclassical Ir(III)(η^2 -H₂) intermediates, according to B3LYP calculations²⁴², with a dissociative pathway involving initial loss of H₂, followed by C-H addition kinetically favoured. ONIOM

calculations²⁴³ on $\text{RuHCl}[(\text{Bu}_2\text{PCH}_2\text{CH}_2)\text{-}^t\text{Bu}(\text{E})\text{-CH}=\text{CH})\text{CH}_2\text{P}^t\text{Bu}_2]$, $\text{RuHCl}(\text{Py})[(\text{Bu}_2\text{PCH}_2\text{-CH}_2)\text{-}^t\text{Bu}\text{-}(\text{E})\text{-CH}=\text{CH})\text{CH}_2\text{PBu}_2]$, $\text{RuCl}(\text{CO})[\text{CH}(\text{C}_2\text{H}_4\text{P}^t\text{Bu}_2)_2]$ and $\text{RuH}(\text{CO})[\text{CH}(\text{C}_2\text{H}_4\text{PBu}_2)_2]$ have been used to show that the bulky P^tBu_2 groups are responsible for the electronically unfavorable cis arrangement of the CO and Cl and to locate the transition state structures for the intramolecular olefin insertion into the Ru-H bond.

Hydrogen scrambling in $[\text{CpOs}(\text{PH}_2\text{CH}_2\text{PH}_2)(\text{CH}_3)\text{H}^*]$ and $[\text{Cp}^*\text{Os}(\text{PMe}_2\text{CH}_2\text{PMe}_2)(\text{CH}_3)\text{H}]^+$ takes place *via* the H-exchange mechanism, reveals a B3YLP and B3LYP:HF ONIOM study²⁴⁴. The first step of this reaction is the C-H* bond formation that takes place *via* a three-centered transition state. After formation of the methane complex, it isomerises and the reverse process occurs, *via* methane C-H bond activation. Methane loss from $\text{TpPtMe}(\text{H})_2$ (Tp = hydrido-tris(pyrazolyl)borate), studied at the mPW1k level²⁴⁵, cannot occur due to the rigidity of the Tp ligand, which does not allow the required trans geometry. H/D scrambling of the methyl ligand is, however, relatively facile and proceeds through a $\eta^2\text{-CH-CH}_4$ complex. Hydrogenation of the double bond in $[\text{CsCl}(\text{H}_2)(\text{PPh}_3)\{\text{Ph}_2\text{P}(\text{CH}_2)_2\text{CH}=\text{CH}(\text{CH}_2)_2\text{PPh}_3\}]\text{OTf}$ is predicted to be thermodynamically feasible but kinetically unfavourable by B3LYP calculations²⁴⁶.

mer,trans- $[(\text{PMe}_3)_3\text{Rh}(\text{-C}\equiv\text{C-R})_2\text{H}]$ from $[(\text{PMe}_3)_4\text{Rh}(\text{Me})]$ and terminal alkyne involves initial elimination of methane and the formation of the trigonal bipyramidal complex $[(\text{PMe}_3)_4\text{Rh}(\text{-C}\equiv\text{C-R})]$, a BP86 study reveals²⁴⁷. This intermediate undergoes an oxidative addition reaction with a second equivalent of alkyne to give *fac*- $[(\text{PMe}_3)_3\text{Rh}(\text{-C}\equiv\text{C-R})_2\text{H}]$ as the kinetic product. The oxidative addition of a Pt(0) fragment, $\text{Pt}(\text{PH}_3)_2$, to one of the rim C-C bonds of semi-buckminsterfullerene ($\text{C}_{30}\text{H}_{12}$), to give an $\eta^2\text{-}\sigma$ -bonded Pt(II)-buckybowl complex has been compared at the BP86 level²⁴⁸ to oxidative addition to the C-C bond in five-membered rings of less strained hydrocarbons to study the effect of ring strain and curvature. The bowl-like curvature of semi-buckminsterfullerene plays an essential role in the C-C bond-breaking reaction, while no attainment of aromaticity is involved in the process. The dirhodium tetracarboxylate-catalysed C-H bond activation/C-C bond formation reaction of a diazo compound with an alkane, studied at the B3LYP level²⁴⁹, is initiated by complexation between of the diazo compound to the rhodium catalyst with N_2 extrusion to give a carbene complex driven by back-donation from the Rh $4d_{xz}$ orbital to the C-N σ^* -orbital. The C-H activation/C-C formation proceeds in a single step through a three-centered hydride transfer-like transition state with a small activation energy. The dehydrogenation of cyclohexadiene and 9,10-dihydroanthracene by *trans*- $(\text{DMPE})_2\text{Ru}(\text{H})(\text{NH}_2)$ to yield benzene (or anthracene), $(\text{DMPE})_2\text{Ru}(\text{H})(2)$, and ammonia has been studied using B3LYP calculations²⁵⁰ suggesting that the NH_2 group is exceptionally basic and prefers to extract a proton from C-H rather than a H atom. Oxidation of the hydrocarbons methane, ethane, methyl fluoride, and ethylene catalysed by *cis*- $(\text{H}_2\text{O})(\text{NH}_2)\text{Fe}(\mu\text{-O})_2(\eta^2\text{-HCOO})_2\text{Fe}(\text{NH}_2)(\text{H}_2\text{O})$ and *cis*- $(\text{HCOO})(\text{Imd})\text{Fe}(\mu\text{-O})_2(\eta^2\text{-HCOO})_2\text{Fe}(\text{Imd})(\text{HCOO})$ start by coordination of the substrate molecule to the bridging oxygen atom followed by the H-atom abstraction, according to B3LYP calculations²⁵¹. The selectivity of C-H activation of R-H by $\text{Ti}(\text{OR}')_2(=\text{NR}')$ is determined by the structure and ener-

getics of the substrate/Ti-imido interaction, according to B3LYP calculations²⁵². The hydride/ η^2 -Si-H hydrogen exchange observed in the bis(silane) complexes $\text{RuH}_2[(\eta^2\text{-HSiMe}_2)_2(\text{CH}_2)_2](\text{PCY}_3)_2$ and $\text{RuH}_2[(\eta^2\text{-HSiPh}_2)_2\text{O}](\text{PCY}_3)_2$ proceed through formation of isomers with dihydrogen ligands, according to NMR and B3LYP studies²⁵³. A B3LYP study²⁵⁴ of methyl-Pd heterocyclic silylene and germylene complexes reveals a very low activation barrier for methyl migration to the silylene or germylene ligand, but indicates that, in the absence of solvent or counterion effects, reductive elimination of silicenium or germacenium cations is less likely.

A B3LYP, B3PW91 and MP2 study²⁵⁵ reveals that Rh-catalysed alkane borylation proceeds *via* formation of a reactive boryl intermediate followed by C-H bond activation and B-C bond formation. Rh-catalysed hydrosilylation of ethylene, studied at the B3LYP, MP4-(SDQ) and CCSD(T) levels²⁵⁶, proceeds with the rate-determining step in the Chalk-Harrod mechanism being Si-C reductive elimination. The apical site of the palladium complex on elementary reactions acts to significantly lower the energy barrier for the oxidative addition of the C-X (X = Sn, Ge, Si, C) bonds of heteroles to the Pd of $(\text{H}_2\text{PC}_2\text{H}_4\text{PH}_2)\text{Pd}$ and the insertion of XH_2 into the Pd-C bond of $(\text{H}_2\text{PC}_2\text{H}_4\text{PH}_2)\text{Pd}(\eta^2\text{-HC=CH})$, according to a B3LYP study²⁵⁷. The catalysis by bis(alkynyl)(1,5-cyclooctadiene)platinum complexes of the cross-linking of polyorganosiloxanes containing Si-H and vinyl groups could proceed *via* two possible mechanisms, according to a BP86 study²⁵⁸. The first one involves a sequence of four oxidative additions and reductive eliminations, while the second one requires a reductive coupling that is induced by olefin coordination. In both cases, the initial step is rate-determining. A B3LYP study²⁵⁹ of the decomposition of a novel palladium-methyl complex of the rigid CNC ligand 2,6-bis(1-alkylimidazol-2-ylidene-3-yl)pyridine predicts that reductive elimination to give 2-methylimidazolium species is a facile reaction.

The mechanism for the activation of the O-H bond in H_2O , the C-H of CH_4 , and the H-H of H_2 , and the π bonds in C_2H_2 , C_2H_4 , and H is significantly affected by the electronic nature of the $\text{Pd}=\text{X}$ bond, according to B3LYP calculations²⁶⁰. Activation of O-H is heterolytic when X = Sn or Si but homolytic for X = C whereas activation of C-H and H-H bonds is heterolytic for all X. Activation of CC double and triple bonds is homolytic for X = Sn whereas activation of the C=O π can proceed *via* homolytic or heterolytic pathways. The rate determining step in the Rh(I)-catalysed intramolecular coupling of an alkenyl group to a C-H bond of a substituted benzimidazole involves insertion of the alkenyl double bond into the rhodium-carbene bond, according to B3LYP calculations²⁶¹. The conversion of methane to methyl bisulfate using $\text{Pt}(\text{NH}_3)_2\text{Cl}_2$ and $\text{Pt}(\text{bpym})\text{Cl}_2$ involves a series of steps beginning with C-H activation to form an intermediate ion-pair $\text{Pt}(\text{II})\text{-CH}_4$ methane complex prior to forming a $\text{Pt}(\text{II})\text{-CH}_3$ complex, a B3LYP study reveals²⁶². The oxidation step is rate determining and is more favourable for the ammine catalyst suggesting higher activity than the bipyrimidine catalyst.

The three step zirconium-catalysed oxidation of amines in the presence of hydroperoxides to give the corresponding nitro compounds proceeds *via* N-

oxides, hydroxylamines and nitroso intermediates, according to a B3LYP study²⁶³. BP86 and Car-Parrinello simulations²⁶⁴ have been used to study the stepwise migratory insertion of methyl isocyanide into the zirconium-carbon bonds in [calix[4](OMe)₂(O)₂-ZrMe₂] showing that methyl isocyanide insertion takes place *via* the initial formation of an η^1 -iminoacyl species that is suddenly converted into the more stable η^2 -isomer. Insertion of the residual alkyl group into the iminoacyl moiety leading to an η^2 -bound imine is then kinetically favoured. A similar approach has also been used²⁶⁵ to study the acetylene to vinylidene isomerization in (Cp)(CO)₂Mn(HC≡CH). The direct 1,2 hydrogen shift, proceeding *via* an agostic intermediate, is predicted to be the energetically most favourable path. The same methodology²⁶⁶ has been applied to migratory insertion using the cationic Ni(II) [(dppp)Ni(CH₃)(CO)]⁺ complex which takes place *via* a five-coordinate complex is thermodynamically and kinetically favoured and methyl attack on the resting carbonyl group.

The alkyl group migration reaction CH₃Co(CO)₄ → CH₃(CO)Co(CO)₃, studied at the B3LYP level²⁶⁷, involves two stable 16-electron acyl intermediates with the carbons of the acyl groups in the axial position. One of the intermediates is stabilized by the formation of an agostic interaction to the formally vacant site of the trigonal bipyramid, and the other is stabilized by the acyl oxygen adopting an η^2 coordination geometry. The carbonyl association reaction CH₃(CO)Co(CO)₃ + CO → CH₃(CO)Co(CO)₄ proceeds *via* methyl migration. Insertion into the C(aryl)-S and not the C(vinyl)-S bond of (η^6 -benzothiophene)Mn(CO)₃⁺ is favoured and η^1 -S coordination of benzothiophene to Mn(CO)₄⁻ is viable in an intermediate in the C-S insertion reactions, according to B3LYP calculations²⁶⁸. Insertion reactions of alkynes (RC≡CR': R = H, R' = H, Me, CF₃, Ph; R = Me, R' = Ph; R = CO₂H, R' = H, Me, CF₃, Ph) with the model phosphanickelacycle [NiBr(CH=CHCH₂PH₂-KCP)(PH₃)] proceed *via* associative processes with 5-coordinate intermediates preferred, a BP86 study has revealed²⁶⁹. B3LYP calculations²⁷⁰ on the C-S cleavage reaction in the thermal degradation of tris(3,5-dimethylpyrazolyl)hydridoboratorhenium(V)(oxo)-(1,2-dithiolate) and -(1,2-monothiodiolate) reveals that substitution of each sulfur raises the predicted activation energy significantly.

An MP2 and B3LYP study²⁷¹ on the tautomers [Ru{=C=C=C(H)CH₃}(η^5 -C₅H₅)(PH₃)₂]⁺ and [Ru{=C=C(H)CH=CH₂}(η^5 -C₅H₅)(PH₃)₂]⁺ predicts that the latter is only slightly more stable than the former and that the spontaneous tautomerization process between both complexes involves a [1,3]-hydrogen sigmatropic rearrangement. A B3LYP study²⁷² of the reaction of a 1,3-diphosphacyclobutane -2,4-diyl-2-ide with chromium or tungsten hexacarbonyl suggests that formation of the anionic complexes [cyclo{P(Mes*)-C(SiMe₃)-P(Mes*)-C(O)-C[M(CO)₅]}]⁻ proceeds by the formal insertion of CO into the four membered ring *via* two intermediates that can be formulated as a cyclic metal acyl and an acyclic ketenyl complex.

3.2.3 Addition Reactions. The oxidative addition of SiH₄ to a platinum-diphosphine complex, Pt(PH₃)₂ has been studied at the BPW91 and dynamic Car-Parrinello levels²⁷³ indicating that the oxidative addition is both thermodynamically

cally and kinetically favoured and takes place *via* a reactant-like transition state leading directly to the more thermodynamically stable *cis*-[PtH(PH₃)₂-SiH₃] square-planar product. The displacement of the MeB(C₆F₅)₃⁻ anion from seven different zirconocene methyl cations by neutral Lewis bases, such as dimethylaniline, benzyldimethylamine, and diⁿbutyl ether, studied at the BP86 level²⁷⁴, proceeds by way of an associative mechanism involving a five-coordinated intermediates with the Lewis base coordinated to the central coordination site. SiH₄ activation by Cp₂LnH complexes has been studied at the B3PW91 level of theory²⁷⁵ and compared to the reactivity of CH₄. Formation of Cp₂Ln(SiH₃) can occur *via* H/H exchange and silylation and both occur *via* a single-step σ -bond metathesis mechanism. Both pathways are therefore thermally accessible with the H/H exchange path more kinetically favourable and the silylation reaction thermodynamically preferred. The considerably lower activation barrier for silylation relative to methylation is attributed to the ability of Si to become hypervalent. The silyl migration reaction of ORe[N(SiMe₂CH₂PCy₂)₂] to give NRe[O(SiMe₂CH₂PCy₂)₂] is driven by greater thermodynamic stability of the latter according to DFT calculations²⁷⁶. The bis-silylation reaction of alkynes by palladium complexes, modelled using Pd(PH₃)₂, studied at the B3LYP level²⁷⁷, proceed by oxidative addition involving H₃Si-SiH₃ to the catalyst leading to *cis*-(SiH₃)₂Pd(PH₃)₂ and transfer of the two silyl groups to the alkyne C-C triple bond in a many step process involving the formation of two C-Si bonds.

The diastereoselectivity of the oxyfunctionalization in the epoxidation of stereolabeled methyl-substituted chiral allylic alcohols, studied at the B3LYP level²⁷⁸, is due to the competition between allylic strain and the electronic advantage for the spiro transition state. The most favourable pathway for the hydroboration reaction of olefins catalysed by Cp₂Ti(HBcat') involves coordination of an olefin to an intermediate with a five-membered ring with a Ti-H-B bridging unit, according to a B3LYP study²⁷⁹. B-H bond cleavage then occurs to allow the reductive elimination to form alkylboronate ester as the main product.

An isolated Au₁₀ cluster should be able to catalyse the CO oxidation reaction even below room temperature according to DFT calculations²⁸⁰ due to special reaction geometries available for small particles in combination with an enhanced ability of low coordinated gold atoms to interact with molecules from the surroundings.

The rhodium(III)-catalysed hydrogenation of carbon dioxide into formic acid has been studied at the B3LYP level²⁸¹ using *cis*-[RhH₂(PH₃)₃]⁺ and *cis*-[RhH₂(PH₃)₂(H₂O)]⁺ model catalysts. The reaction proceeds by initial CO₂ insertion into the Rh(III)-H bond followed by either by isomerization of [RhH(η^1 -OCOH)(PH₃)₂(H₂O)]⁺, five-centered H-OCOH reductive elimination and oxidative addition of H₂ to [Rh(PH₃)₂(H₂O)]⁺ or through isomerization of [RhH(η^1 -OCOH)(PH₃)₂(H₂O)(H₂)]⁺ and six-centered σ -bond metathesis of [RhH(η^1 -OCOH)(PH₃)₂(H₂O)]⁺ with H₂. A B3LYP study²⁸² reveals that hydrogen transfer from the dihydrogen to the norbornadiene ligand of [Ru(H₂)(norbornadiene)(2,6-(Ph₂PCH₂)₂C₆H₃)]⁺ proceeds through a stepwise mechanism. A B3PW91 study²⁸³ of ether dehydrogenation by [RuHCl(P'Pr₃)₂]₂ suggests that

coordination of the removed H_2 is essential for reaction thermodynamics.

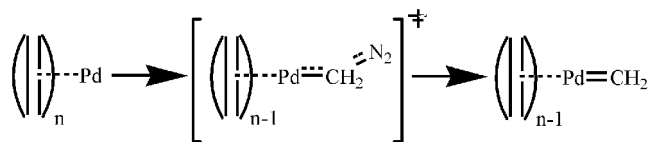
The regioselectivity of nucleophilic attack in silyl-substituted (diphosphino)(η^3 -allyl)palladium cations has been studied at the B3LYP level²⁸⁴. For unsymmetrical allyl ligands the shortest Pd-C(terminal) bond is the one corresponding to the carbon atom directly bonded to silicon, electronic factors being determinant. When the silicon group is the bulkiest one, both steric and electronic factors favour the attack at the carbon atom remote from silicon (γ -carbon). When the silicon substituent is the least sterically demanding, the attack at carbon bonded to silicon (α -carbon) is sterically more favorable, but electronic effects favor the attack at the γ -carbon.

The Pt(PPh₃)₂-catalysed reaction between disilacyclobutene and acetylene proceeds *via* oxidative addition of the Si-Si bond of disilacyclobutene to Pt, release of one phosphine ligand, coordination of acetylene to form a π -complex, migratory insertion of acetylene into a Pt-Si bond leading to an Si-C bond, coordination of acetylene, and elimination of product disilacyclohexadiene, a B3LYP study reveals²⁸⁵. The rate-determining step is the insertion of acetylene into a Pt-Si bond.

B3LYP calculations²⁸⁶ suggest that reaction of Mo(PMe₃)₆ with 2,6-Ph₂C₆H₃OH to give the η^6 -arene complex [η^6 -C₆H₅C₆H₃(Ph)OH]Mo(PMe₃)₃ proceeds *via* oxidative addition of the O-H bond to give a non-classical Mo...H-OAr hydrogen bond. A B3LYP study²⁸⁷ of the reductive elimination of methane from *cis*, *trans*-Os(H)₂(CH₃)(NO)L₂ (L = PⁱPr₃) with and without LiNMe₂ show the experimentally observed rate acceleration is due to preferential stabilization of the oxidative addition transition state, due to the greater back donation to NO possible because of the relief of the filled-filled repulsion between the occupied Os d and C-H σ -orbitals by the Li electrophile on NO oxygen.

3.2.4 Cyclization and Metathesis Reactions. BP86 calculations²⁸⁸ have been used to study alternative mechanisms of the metathesis reactions between ethene and model catalysts [(PH₃)(L)Cl₂Ru=CH₂] (L = PH₃ and imidazol-2-ylidene). Initial addition of ethene is rate-determining on the associative pathway but ring closure to yield a ruthenacyclobutane, or its reverse, is rate determining on the dissociative pathway. Pathways for the reaction of ethene with diazomethane to produce cyclopropane and dinitrogen catalysed by Pd(0) complexes have been investigated at the B3LYP level²⁸⁹ leading to an activation energy of 71.7 kJ mol⁻¹ for the most favorable catalytic cycle, far lower than previously reported computed barriers for Pd(II)-catalysed pathways of this reaction. Pd(η^2 -C₂H₄)₂ is predicted to be the resting state of the catalyst, in equilibrium with Pd(η^2 -C₂H₄)(κ -C-CH₂N₂), from which N₂ is eliminated in the rate-determining step 7. The cyclopropanation reactions with ethylene of several mono zinc carbenoids proceed *via* an asynthchronous attack on one CH₂ whilst the corresponding gem-dizinc carbenoids proceed *via* synchronous attack on both CH₂ groups, according to B3LYP calculations²⁹⁰. The charges on the carbon atoms and protons in Hg(C₆H₆)₂(AlCl₄)₂ and [Hg(C₆H₆)₂(AlCl₄)]⁺ at the DFT level²⁹¹ are significantly higher than in uncomplexed benzene or HgCl₂(C₆H₆)₂ so that proto-

nation of benzene is thermodynamically favoured in comparison to protonation of benzene by HO_2CCF_3 , a known catalyst for arene H/D exchange. The reaction of allene with carbon dioxide using $[\text{RhCl}(\text{C}_2\text{H}_4)(\text{P}^i\text{Pr}_3)_2]$ as catalyst has been studied at the B3LYP level²⁹² and leads to a four membered lactone.



7

A comprehensive investigation²⁹³ using BP86 calculations and hybrid BP86 / MM calculations on the influence of the ligand L on the regulation of the product selectivity for the $[\text{Ni}^0\text{L}]$ -catalysed cyclodimerization of 1,3-butadiene show that allylic isomerization, allylic enantioface conversion and oxidative coupling are influenced to a minor extent by electronic and steric effects. The steric bulk on the ligand as well as its π -acceptor ability act to facilitate the reductive elimination, while σ -donor abilities serve to retard this process. A similarly comprehensive investigation of the mechanism for cyclodimerization of butadiene by the generic $[\text{bis}(\text{butadiene})(\text{Ni}^0\text{PH}_3)]$ at the BP86 level²⁹⁴. Starting from a pre-established equilibrium between several configurations of the $[(\text{octadienediyl})(\text{Ni}^{\text{II}}\text{L})]$ complex, the major cyclodimer products are formed along competing reaction paths *via* reductive elimination, as the overall rate-determining step. BP86 calculations²⁹⁵ have been used to computational screen late-transition-metal catalysts and nitrogen-containing polar monomers toward an incorporation of amines and nitriles in the polymer chain of polyolefins. The calculations reveal the general trend that the activation energies for the ethylene, propylene, and acrylonitrile insertion in the Brookhart systems are similar, whereas the activation energies for the vinylamine insertion are much higher. A similar approach²⁹⁶ has also been used for an initial screening of late-transition-metal catalysts and nitrogen-containing polar monomers toward an incorporation of amines or nitriles in the polymer chain of polyolefins. Substrates of the type $\text{CH}_2 = \text{CH}(\text{CH}_2)_n\text{X}$ ($\text{X} = \text{polar group}$) can bind either with the N-containing polar group or with the π moiety to the metal centre of the catalyst, with the latter leading to polymer growth.

The activity of the catalyst in vinyl-vinyl reductive elimination reaction from bis- σ -vinyl complexes $[\text{M}(\text{CH}=\text{CH}_2)_2\text{X}_n]$, studied at the B3LYP level²⁹⁷, decreases in order $\text{Pd}^{\text{IV}}, \text{Pd}^{\text{II}} > \text{Pt}^{\text{IV}}, \text{Pt}^{\text{II}}, \text{Rh}^{\text{III}} > \text{Ir}^{\text{III}}, \text{Ru}^{\text{II}}, \text{Os}^{\text{II}}$. The activation mechanism of the π bonds, the nonpolar $\text{C}\equiv\text{C}$ of C_2H_2 and the polar $\text{C}=\text{O}$ of HCHO and the $\text{C}=\text{N}$ of HCN at the $\text{Pd}=\text{Sn}$ bond of the model complex $(\text{H}_2\text{PC}_2\text{H}_4\text{PH}_2)\text{-Pd}=\text{SnH}_2$ has been studied at the B3LYP level²⁹⁸. For the non-polar ethyne $\text{C}\equiv\text{C}$ and $\text{C}=\text{N}$ π bond, the reaction proceeds by the homolytic mechanism supported by the rotation of the $(\text{H}_2\text{PC}_2\text{H}_4\text{PH}_2)\text{Pd}$ group around the Pd-Sn axis. For the strongly polarized formaldehyde $\text{C}=\text{O}$ π bond, the donation of lone pair electron on the $\text{C}=\text{O}$ oxygen to the Sn p orbital is so strong that the $\text{C}=\text{O}$ bond is broken by the heterolytic mechanism with the electrophilic attack

of the C=O carbon to the Pd atom and rotation is not necessary.

The reaction of nickel dithiolene complexes and ethylene, studied at the B3LYP level²⁹⁹, is a two-step process, in which a trans-product forms first which then rearranges to the more thermodynamically stable cis-product. The syntheses of helicenes based on the modular assembly of key cis,cis-dienetriynes and their nickel(0)-catalysed [2+2+2] cycloisomerization strongly favour the intramolecular simultaneous construction of three aromatic rings, according to B3LYP calculations³⁰⁰.

BP86 calculations³⁰¹ on the ruthenium-catalysed olefin metathesis reactions involving a Grubbs-type (PCy₃)₂-Cl₂Ru=CHPh catalyst and a heteroleptic (pre)catalytic system, in which a *N*-heterocyclic carbene, NHC, ligand substitutes a single phosphine, predict that both the PCy₃-Ru binding and the insertion barrier are lower for heteroleptic system.

Endo- and exo-cycloisomerizations of 4-pentyn-1-ol using a tungsten pentacarbonyl catalyst, proceeds with a rate-determining C_α-C_β hydride migration step to form a vinylidene intermediate, according to a B3LYP study³⁰², with the primary role of the tungsten catalyst being to stabilize the vinylidene intermediate. The thermodynamic products of the reaction between ethyne and the model compounds (HE)₃M = M(EH)₃ (M = Mo and W; E = O and S) are the alkyne adducts M₂(μ-C₂H₂)(EH)₆ rather than metathesis products HC = M(EH)₃, except when M = W and E = O according to a B3LYP study³⁰³.

The role of the zinc catalyst in the Diels-Alder reaction between cyclopentadiene and 3-phenyl-1-(2-pyridyl)-2-propen-1-one has been studied at the B3LYP level³⁰⁴. The uncatalysed process proceeds *via* an asynchronous concerted [4+2] reaction but the presence of a Lewis acid catalyst changes the mechanism drastically into a polar stepwise process. The mechanism of cyclopropanation, catalysed by a 3-oxobutylideneaminatocobalt(II) complex, has been analysed at the B3LYP level³⁰⁵. The axial donor ligand on the catalyst reduces the activation energy for formation of the cobalt carbene complex but increases the activation energy for the cyclopropanation step.

References

1. W. Scherer, P. Sirsch, D. Shorokhov, G.S. McGrady, S.A. Mason and M.G. Gardiner, *Chem. – Eur. J.*, 2002, **8**, 2324.
2. J.K. Parker and H.H. Nelson, *Chem. Phys. Lett.*, 2002, **360**, 313.
3. N.W. Mitzel, C. Lustig, R.J.F. Berger and N. Runeberg, *Angew. Chem. Int. Ed. Engl.*, 2002, **41**, 2519.
4. R. Becerra, S.E. Boganov, M.P. Egorov, V.I. Faustov, I.V. Krylova, O.M. Nefedov and R. Walsh, *J. Am. Chem. Soc.*, 2002, **124**, 7555.
5. C. Lustig and N.W. Mitzel, *Organometallics*, 2002, **21**, 3471.
6. G. Vass, G. Tarczay, G. Magyarfalvi, A. Bodi and L. Szepes, *Organometallics*, 2002, **21**, 2751.
7. Y.J. Kang, D.Y. Song, H. Schmider and S.N. Wang, *Organometallics*, 2002, **21**, 2413.
8. H.M. Badawi and Z.S. Seddigi, *J. Mol. Struct. Theochem.*, 2002, **578**, 181.
9. A. Kuczkowski, S. Schulz, M. Nieger and P.R. Schreiner, *Organometallics*, 2002, **21**,

- 1408.
10. K. Tani, R. Yamada, T. Kanda, M. Suzuki, S. Kato and T. Murai, *Organometallics*, 2002, **21**, 1487.
 11. H. Fleischer, B. Mathiasch, D. Schollmeyer, *Organometallics*, 2002, **21**, 526.
 12. R. Tacke, T. Schmid, C. Burschka, M. Penka and H. Surburg, *Organometallics*, 2002, **21**, 113.
 13. P. Avalle, R.K. Harris and R.D. Fischer, *Phys. Chem. Chem. Phys.*, 2002, **4**, 3558.
 14. T.N.P. Luhtanen, M. Linnolahti and T.A. Pakkanen, *J. Organomet. Chem.*, 2002, **642**, 49.
 15. G. Cretiu, L. Silaghi-Dumitrescu, L. Silaghi-Dumitrescu, J. Escudie, A. Toscano, S. Hernandez and R. Cea-Olivares, *J. Organomet. Chem.*, 2002, **659**, 95.
 16. P. Avalle, R.K. Harris, P.B. Karadakov and P.J. Wilson, *Phys. Chem. Chem. Phys.*, 2002, **4**, 5925.
 17. H. Lange, U. Herzog, U. Bohme and G. Rheinwald, *J. Organomet. Chem.*, 2002, **660**, 43.
 18. F. Haeffner, P. Brandt and R.E. Gawley, *Org. Lett.*, 2002, **4**, 2101.
 19. C.J. Barden, P. Charbonneau and H.F. Schaefer, *Organometallics*, 2002, **21**, 3605.
 20. G.D. Geske and A.I. Boldyrev, *Inorg. Chem.*, 2002, **41**, 2795.
 21. J. Campbell, H.P.A. Mercier, H. Franke, D.P. Santry, D.A. Dixon and G.J. Schrobilgen, *Inorg. Chem.*, 2002, **41**, 86.
 22. A. Stasch, M. Ferbinteanu, J. Prust, W.J. Zheng, F. Cimpoesu, H.W. Roesky, J. Magull, H.G. Schmidt and M. Noltemeyer, *J. Am. Chem. Soc.*, 2002, **124**, 5441.
 23. W.H. Lam and Z.Y. Lin, *Polyhedron*, 2002, **21**, 503.
 24. E.S. Shubina, E.V. Bakhmutova, A.M. Filin, I.B. Sivaev, L.N. Teplitskaya, A.L. Chistyakov, I.V. Stankevich, V.I. Bakhmutov, V.I. Bregadze and L.M. Epstein, *J. Organomet. Chem.*, 2002, **657**, 155.
 25. C. Bauer, D. Gabel, T. Borrmann, J.D. Kennedy, C.A. Kilner, M. Thornton-Pett, U. Dorfler, *J. Organomet. Chem.*, 2002, **657**, 205.
 26. M. Hofmann and S.K. Goll, *J. Organomet. Chem.*, 2002, **657**, 257.
 27. R. Vivas-Reyes, F. De Proft, P. Geerlings, M. Biesemans, R. Willem, F. Ribot and C. Sanchez, *New. J. Chem.*, 2002, **26**, 1108.
 28. T.P. Hanusa, *Organometallics*, 2002, **21**, 2559.
 29. J.D. Smith and T.P. Hanusa, *Organometallics*, 2002, **21**, 1518.
 30. V.M. Rayon and G. Frenking, *Chem. – Eur. J.*, 2002, **8**, 4693.
 31. R.W. Schurko, I. Hung, C.L.B. Macdonald and A.H. Cowley, *J. Am. Chem. Soc.*, 2002, **124**, 13204.
 32. C.A. Morrison, D.S. Wright and R.A. Layfield, *J. Am. Chem. Soc.*, 2002, **124**, 6775.
 33. A. Terheiden, B. Bernhardt, H. Willner and F. Aubke, *Angew. Chem. Int. Ed. Engl.*, 2002, **41**, 799.
 34. M.F. Zhou, N. Tsumori, Z.H. Li, K.N. Fan, L. Andrews, and Q.A. Xu, *J. Am. Chem. Soc.*, 2002, **124**, 12936.
 35. H. Bornemann and W. Sander, *J. Organomet. Chem.*, 2002, **641**, 156.
 36. S.C. Farantos, E. Filippou, S. Stamatidis, G.E. Froudakis, M. Mulhauser, M. Massaouti, A. Sfounis and M. Velegrakis, *Chem. Phys. Lett.*, 2002, **366**, 231.
 37. A.J. Downs, H.J. Himmel and L. Manceron, *Polyhedron*, 2002, **21**, 473.
 38. M. Weidenbruch, *J. Organomet. Chem.*, 2002, **646**, 39.
 39. B. Bonelli, B. Civalieri, P. Ugliengo, Z. Gabelica and E. Garrone, *Phys. Chem. Chem. Phys.*, 2002, **4**, 1658.
 40. M. Reiher and A. Sundermann, *Eur. J. Inorg. Chem.*, 2002, **7**, 1854.
 41. A.Y. Timoshkin and G. Frenking, *J. Am. Chem. Soc.*, 2002, **124**, 7240.

42. C.H. Lai, M.D. Su and S.Y. Chu, *Polyhedron*, 2002, **21**, 579.
43. U.D. Priyakumar and G.N. Sastry, *J. Org. Chem.*, 2002, **67**, 271.
44. N. Nakata, N. Takeda and N. Tokitoh, *J. Am. Chem. Soc.*, 2002, **124**, 6914.
45. G. Frison and A. Sevin, *J. Organomet. Chem.*, 2002, **643**, 105.
46. D. Delaere, M.T. Nguyen and L.G. Vanquickenborne, *J. Organomet. Chem.*, 2002, **643**, 193.
47. A. Fekete and L. Nyulaszi, *J. Organomet. Chem.*, 2002, **643**, 278.
48. D. Scheschkewitz, M. Hofmann, A. Ghaffari, P. Amseis, C. Prasang, W. Mesbah, G. Geiseler, W. Massa and A. Berndt, *J. Organomet. Chem.*, 2002, **646**, 262.
49. L.E. Guseľnikov, V.V. Volkova, E.N. Buravtseva, A.S. Redchin, N. Auner, B. Herrschaft, B. Solouki, G. Tsantes, Y.E. Ovchinnikov, S.A. Pogozhikh, F.M. Dolgushin and V.V. Egrebetsky, *Organometallics*, 2002, **21**, 1101.
50. M. Bendikov, B. Solouki, N. Auner and Y. Apeloig, *Organometallics*, 2002, **21**, 1349.
51. M. Takahashi and K. Sakamoto, *Organometallics*, 2002, **21**, 4212.
52. H.J. Himmel, L. Manceron, A.J. Downs and P. Pullumbi, *J. Am. Chem. Soc.*, 2002, **124**, 4448.
53. P.V. Bharatam, R. Moudgil and D. Kaur, *Organometallics*, 2002, **21**, 3683.
54. M. Yoshida and N. Tamaoki, *Organometallics*, 2002, **21**, 2587.
55. U.D. Priyakumar and G.N. Sastry, *Organometallics*, 2002, **21**, 1493.
56. U.D. Priyakumar, D. Saravanan and G.N. Sastry, *Organometallics*, 2002, **21**, 4823.
57. N. Takeda, A. Shinohara and N. Tokitoh, *Organometallics*, 2002, **21**, 4024.
58. N. Takeda, A. Shinohara and N. Tokitoh, *Organometallics*, 2002, **21**, 256.
59. N. Tokitoh, K. Hatano, T. Sasaki, T. Sasamori, N. Takeda, N. Takagi and S. Nagase, *Organometallics*, 2002, **21**, 4309.
60. K.W. Henderson, A.R. Kennedy, D.J. MacDougall and D. Shanks, *Organometallics*, 2002, **21**, 606.
61. M.L. Helm, P.B. Hitchcock, J.F. Nixon, L. Nyulaszi and D. Szieberth, *J. Organomet. Chem.*, 2002, **659**, 84.
62. W. Nakanishi and S. Hayashi, *J. Org. Chem.*, 2002, **67**, 38.
63. J. Ma, A. Hozaki and S. Inagaki, *Inorg. Chem.*, 2002, **41**, 1876.
64. A.I. Boldyrev and A.E. Kuznetsov, *Organometallics*, 2002, **21**, 532.
65. S.M. Bachrach, *J. Organomet. Chem.*, 2002, **643**, 39.
66. M.J. Huang and M.D. Su, *J. Organomet. Chem.*, 2002, **659**, 121.
67. N.J. Mosey, K.M. Baines and T.K. Woo, *J. Am. Chem. Soc.*, 2002, **124**, 13306.
68. M. Bendikov, S.R. Quadt, O. Rabin and Y. Apeloig, *Organometallics*, 2002, **21**, 3930.
69. M.D. Su, *J. Am. Chem. Soc.*, 2002, **124**, 12335.
70. N. Al-Rubaiey, R. Becerra and R. Walsh, *Phys. Chem. Chem. Phys.*, 2002, **4**, 5072.
71. R. Becerra, S.E. Boganov, M.P. Egorov, V.I. Faustov, V.M. Promyslov, O.M. Nefedov and R. Walsh, *Phys. Chem. Chem. Phys.*, 2002, **4**, 5079.
72. B.H. Boo, N. Saito, I.H. Suzuki and I. Koyano, *J. Mol. Struct.*, 2002, **610**, 17.
73. N. Ben Amor and C. Daniel, *Coord. Chem. Rev.* 2002, **226**, 11.
74. E. Hupe, P. Knochel and K.J. Szabo, *Organometallics*, 2002, **21**, 2203.
75. K. Yoshizawa, Y. Kondo, S.Y. Kang, A. Naka and M. Ishikawa, *Organometallics*, 2002, **21**, 3271.
76. S. Schmatz, *Organometallics*, 2002, **21**, 864.
77. Q.C. Shi and S. Kais, *J. Am. Chem. Soc.*, 2002, **124**, 11723.
78. Y. Wu, Y.H. Ding, S.M. Li, Z.S. Li and C.C. Sun, *Chem. Phys. Lett.*, 2002, **351**, 267.
79. V. Stert, H.H. Ritze, W. Radloff, K. Gasmi and A. Gonzalez-Urena, *Chem. Phys. Lett.*, 2002, **335**, 449.

80. Y. Wu, Y.H. Ding, J.F. Xiao, Z.S. Li, X.R. Huang and C.C. Sun, *Chem. Phys.*, 2002, **278**, 1.
81. G. Talarico and P.H.M. Budzelaar, *Organometallics*, 2002, **21**, 34.
82. G.A. Olah, A. Torok, J.P. Joscsek, I. Bucusi, P.M. Esteves, G. Rasul and G.K.S. Prakash, *J. Am. Chem. Soc.*, 2002, **124**, 11379.
83. L.E. Gusel'nikov, V.G. Avakyan and S.L. Gusel'nikov, *J. Am. Chem. Soc.*, 2002, **124**, 662.
84. A. Naka, J. Ikadai, S. Motoike, K. Yoshizawa, Y. Kondo, S.Y. Kang and M. Ishikawa, *Organometallics*, 2002, **21**, 2033.
85. C.H. Lai, M.D. Su and S.Y. Chu, *Organometallics*, 2002, **21**, 1320.
86. C.H. Lai, M.D. Su and S.Y. Chu, *Organometallics*, 2002, **21**, 397.
87. M. Cypryk and J. Chojnowski, *J. Organomet. Chem.*, 2002, **642**, 163.
88. D.V. Yandulov, J.C. Huffman and K.G. Caulton, *Organometallics*, 2002, **21**, 4030.
89. P. Macchi, L. Garlaschelli, and A. Sironi, *J. Am. Chem. Soc.*, 2002, **124**, 14173.
90. B. von Ahsen, M. Berkei, G. Henkel, H. Willner and F. Aubke, *J. Am. Chem. Soc.*, 2002, **124**, 8371.
91. P.M. Bradley, M.L. Drummond, C. Turro and B.E. Bursten, *Inorg. Chim. Acta.*, 2002, **334**, 371.
92. J. Handzlik, F. Hartl and T. Szymanska-Buzar, *New. J. Chem.*, 2002, **26**, 145.
93. N.R. Walker and M.C.L. Gerry, *Inorg. Chem.*, 2002, **41**, 1236.
94. L. Maron, L. Perrin, O. Eisenstein and R.A. Andersen, *J. Am. Chem. Soc.*, 2002, **124**, 5614.
95. D. Majumdar, K. Balasubramanian and H. Nitsche, *Chem. Phys. Lett.*, 2002, **361**, 143.
96. E.S. Apostolova, A.P. Tikhonov and O.A. Sendyurev, *Russ. J. Coord. Chem.*, 2002, **28**, 35.
97. A. Vlcek, *Coord. Chem. Rev.*, 2002, **230**, 225.
98. D.M. Dattelbaum, K.M. Omberg, J.R. Schoonover, R.L. Martin and T.J. Meyer, *Inorg. Chem.*, 2002, **41**, 6071.
99. T.J.J. Kinnunen, M. Haukka, E. Pesonen and T.A. Pakkanen, *J. Organomet. Chem.*, 2002, **655**, 31.
100. T.J.J. Kinnunen, M. Haukka and T.A. Pakkanen, *J. Organomet. Chem.*, 2002, **654**, 8.
101. T.E. Bitterwolf, W.B. Scallorn, J.T. Bays, C.A. Weiss, J.C. Linehan, J. Franz and R. Poli, *J. Organomet. Chem.*, 2002, **652**, 95.
102. D. Moigno, I. Pavel, W. Kiefer, H. Jehle and W. Malisch, *J. Organomet. Chem.*, 2002, **648**, 155.
103. P. Norman, P. Cronstrand and J. Ericsson, *Chem. Phys.*, 2002, **285**, 207.
104. B.T. Zhuang, H.F. Sun, L.J. He, Z.F. Zhou, C.S. Lin, K.C. Wu and Z.X. Huang, *J. Organomet. Chem.*, 2002, **655**, 233.
105. S. Frantz, H. Hartmann, N. Doslik, M. Wanner, W. Kaim, H.J. Kummerer, G. Denninger, A.L. Barra, C. Duboc-Toia, J. Fiedler, I. Ciofini, C. Urban and M. Kaupp, *J. Am. Chem. Soc.*, 2002, **124**, 10563.
106. D. Costa, G. Martra, M. Che, L. Manceron and M. Kermarec, *J. Am. Chem. Soc.*, 2002, **124**, 7210.
107. M. Erdmann, O. Rubner, Z. Shen and V. Engel, *J. Organomet. Chem.*, 2002, **661**, 191.
108. T. Bollwein, P.J. Brothers, H.L. Hermann and P. Schwerdtfeger, *Organometallics*, 2002, **21**, 5236.
109. G. Frenking, K. Wichmann, N. Frohlich, J. Grobe, W. Golla, D. Le Van, B. Krebs and M. Lage, *Organometallics*, 2002, **21**, 2921.

110. M.R. Wilson, A. Prock, W.P. Giering, A.L. Fernandez, C.M. Haar, S.P. Nolan and B.M. Foxman, *Organometallics*, 2002, **21**, 2758.
111. K. Krogh-Jespersen, M. Czerw, K.M. Zhu, B. Singh, M. Kanzelberger, N. Darji, P.D. Achord, K.B. Renkema and A.S. Goldman, *J. Am. Chem. Soc.*, 2002, **124**, 10797.
112. M. Bergamo, T. Beringhelli, G. D'Alfonso, P. Mercandelli and A. Sironi, *J. Am. Chem. Soc.*, 2002, **124**, 5117.
113. B.D. Ward, E. Clot, S.R. Dubberley, L.H. Gadeck and P. Mountford, *Chem. Commun.*, 2002, 2618.
114. K.N. Jayaprakash, A.M. Gillepsie, T.B. Gunnoe and D.P. White, *Chem. Commun.*, 2002, 372.
115. A. Knodler, W. Kaim, V.K. Jain and S. Zalis, *J. Organomet. Chem.*, 2002, **655**, 218.
116. A. Klein, J. van Slageren and S. Zalis, *Inorg. Chem.*, 2002, **41**, 5216.
117. G. Sini, O. Eisenstein and R.H. Crabtree, *Inorg. Chem.*, 2002, **41**, 602.
118. M. Doux, C. Bouet, N. Mezailles, L. Ricard and P. Le Floch, *Organometallics*, 2002, **21**, 2785.
119. R.S. Shamsiyev, T.I. Perepelkova, A.A. Mal'kov, I.P. Romm, A.P. Belov, *Russ. J. Coord. Chem.*, 2002, **28**, 104.
120. W.F. Liaw, J.H. Lee, H.B. Gau, C.H. Chen, S.J. Jung, C.H. Hung, W.Y. Chen, C.H. Hu and G.H. Lee, *J. Am. Chem. Soc.*, 2002, **124**, 1680.
121. M. Casarin, L. Pandolfo and A. Sassi, *Organometallics*, 2002, **21**, 2235.
122. N.A. Bokach, V.Y. Kukushkin, M.L. Kuznetsov, D.A. Garnovskii, G. Natile and A.J.L. Pombeiro, *Inorg. Chem.*, 2002, **41**, 2041.
123. M. Zehnder, M. Neuburger, S. Schaffner, M. Jufer and D.A. Plattner, *Eur. J. Inorg. Chem.*, 2002, **6**, 1511.
124. O. Eisenstein and L. Maron, *J. Organomet. Chem.*, 2002, **647**, 190.
125. D.L. Clark, J.C. Gordon, P.J. Hay, R.L. Martin and R. Poli, *Organometallics*, 2002, **21**, 5000.
126. W.K. Seok, H.N. Lee, M.Y. Kim, T.M. Klapotke, Y. Dong and H. Yun, *J. Organomet. Chem.*, 2002, **654**, 174.
127. A. Vyater, C. Wagner, K. Merzweiler and D. Steinborn, *Organometallics*, 2002, **21**, 4369.
128. M.J. Byrnes, M.H. Chisholm, J. Gallucci and P.J. Wilson, *Organometallics*, 2002, **21**, 2240.
129. S. Aime, E. Diana, R. Gobetto, M. Milanesio, E. Valls and D. Viterbo, *Organometallics*, 2002, **21**, 50.
130. P. Belanzoni, M. Rosi and A. Sgamellotti, *J. Organomet. Chem.*, 2002, **648**, 14.
131. L.F. Veiros and M.E.M. da Piedade, *J. Organomet. Chem.*, 2002, **662**, 105.
132. X.Y. Liu, S. Bouherour, H. Jacobsen, H.W. Schmalle and H. Berke, *Inorg. Chim. Acta*, 2002, **330**, 250.
133. C.E. Webster and M.B. Hall, *Inorg. Chim. Acta*, 2002, **330**, 268.
134. M. Steigelmann, Y. Nisar, F. Rominger and B. Goldfuss, *Chem. – Eur. J.*, 2002, **8**, 5211.
135. W.Y. Wong, S.H. Cheung, X. Huang and Z.Y. Lin, *J. Organomet. Chem.*, 2002, **655**, 39.
136. M.H. Chisholm, *J. Organomet. Chem.*, 2002, **641**, 15.
137. S. Aime, F. Bertone, R. Gobetto, L. Milone, A. Russo, M.J. Stchedroff and M. Milanesio, *Inorg. Chim. Acta.*, 2002, **334**, 448.
138. M.J. Bakker, F.W. Vergeer, F. Hartl, P. Rosa, L. Ricard, P. Le Floch and M.J. Calhorda, *Chem. – Eur. J.*, 2002, **8**, 1741.

139. K.A. Bunten, L.Z. Chen, A.L. Fernandez and A.J. Poe, *Coord. Chem. Rev.*, 2002, **233**, 41.
140. L.M. Epstein and E.S. Shubina, *Coord. Chem. Rev.*, 2002, **231**, 165.
141. T.W. Hayton, P. Legzdins and W.B. Sharp, *Chem. Rev.*, 2002, **105**, 925.
142. J. Lee, L. Chen, A.H. West and G.B. Richter-Addo, *Chem. Rev.*, 2002, **102**, 1019.
143. F.F. de Biani, M. Fontani, E. Ruiz, P. Zanello, J.M. Russell and R.N. Grimes, *Organometallics*, 2002, **21**, 4129.
144. J. Frunzke, M. Lein and G. Frenking, *Organometallics*, 2002, **21**, 3351.
145. A.A. Dickinson, D.J. Willock, R.J. Calder and S. Aldridge, *Organometallics*, 2002, **21**, 1146.
146. S.E. d'Arbeloff-Wilson, P.B. Hitchcock, J.F. Nixon and L. Nyulaszi, *J. Organomet. Chem.*, 2002, **655**, 7.
147. X. Sava, M. Melaimi, N. Mezaillies, L. Ricard, F. Mathey and P. Le Floch, *New. J. Chem.*, 2002, **26**, 1378.
148. H.C. Hsu, F.W. Lin, C.C. Lai, P.H. Su and C.S. Yeh, *New. J. Chem.*, 2002, **26**, 481.
149. T.J. Brunker, J.C. Green and D. O'Hare, *Inorg. Chem.*, 2002, **41**, 1701.
150. F. Abu-Hasanayn, P.H.Y. Cheong and M. Oliff, *Angew. Chem. Int. Ed. Engl.*, 2002, **41**, 2120.
151. Y. Oprunenko, I. Gloriovov, K. Lyssenko, S. Malyugina, D. Mityuk, V. Mstislavsky, H. Gunther, G. von Firks and M. Ebener, *J. Organomet. Chem.*, 2002, **656**, 27.
152. A. Vierheilig, D. Moigno, W. Kiefer and A. Materny, *J. Mol. Spectrosc.*, 2002, **211**, 58.
153. M.J. Calhorda, V. Felix and L.F. Veiros, *Coord. Chem. Rev.*, 2002, **230**, 49.
154. I.S. Goncalves, P. Ribeiro-Claro, C.C. Romao, B. Royo and Z.M. Tavares, *J. Organomet. Chem.*, 2002, **648**, 270.
155. M.J. Calhorda, I.S. Goncalves, B.J. Goodfellow, E. Herdtweck, C.C. Romao, B. Royo and L.F. Veiros, *New. J. Chem.*, 2002, **26**, 1552.
156. M.J. Calhorda, C.C. Romao and L.F. Veiros, *Chem. - Eur. J.*, 2002, **8**, 868.
157. J. Llop, C. Vinas, F. Teixidor, L. Victori, R. Kivekas and R. Sillanpaa, *Organometallics*, 2002, **21**, 355.
158. P. Boulet, H. Chermette and J. Weber, *Inorg. Chem.*, 2002, **41**, 7032.
159. C.E. Zachmanoglou, A. Docrat, B.M. Bridgewater, G. Parkin, C.G. Brandow, J.E. Bercaw, C.N. Jardine, M. Lyall, J.C. Green and J.B. Keister, *J. Am. Chem. Soc.*(184) 2002, **124**, 9525
160. W. Malisch, M. Hofmann, M. Nieger, W.W. Scholler and A. Sundermann, *Eur. J. Inorg. Chem.*, 2002, **12**, 3242.
161. J.M. Molina, J.A. Dobado and S. Melchor, *J. Mol. Struct. - Theochem.*, 2002, **589**, 337.
162. M. Kaczorowska and J.N. Harvey, *Phys. Chem. Chem. Phys.*, 2002, **4**, 5227.
163. C. Manzur, M. Fuentealba, L. Millan, G. Gajardo, D. Carrillo, J.A. Mata, S. Sinbandhit, P. Hamon, J.R. Hamon, S. Kahlal and J.Y. Saillard, *New. J. Chem.*, 2002, **26**, 213.
164. C. Lopez, A. Caubet, S. Perez, R. Bosque, X. Solans and M. Font-Bardia, *Polyhedron*, 2002, **21**, 2361.
165. C.V.R. de Moura, R.M. Silva, A. Cesar, M.Y. Darensbourg and J. Reibenspies, *Polyhedron*, 2002, **21**, 2227.
166. A. van der Pol, J.P.C. van Heel, R.H.A.M. Meijers, R.J. Meier and M. Kranenburg, *J. Organomet. Chem.*, 2002, **651**, 80.
167. V. Cavillot and B. Champagne, *Inorg. Chim. Acta*, 2002, **449**, 354.

168. K. Kunz, G. Erker, G. Kehr, R. Frohlich, H. Jacobsen, H. Berke and O. Blacque, *J. Am. Chem. Soc.*, 2002, **124**, 3316.
169. B.F. Johnston, D.W.H. Rankin, H.E. Robertson, R.P. Hughes and J.R. Lomprey, *Organometallics*, 2002, **21**, 4840.
170. O. Kadkin, C. Nather and W. Friedrichsen, *J. Organomet. Chem.*, 2002, **642**, 161.
171. D.V. Deubel, *Organometallics*, 2002, **21**, 4303.
172. J. Eckert, C.E. Webster, M.B. Hall, A. Albinati and L.M. Venanzi, *Inorg. Chim. Acta*, 2002, **330**, 240.
173. M.H. Baik, J.B. Crystal and R.A. Friesner, *Inorg. Chem.*, 2002, **41**, 5926.
174. Y. Li, J.E. McGrady and T. Baer, *J. Am. Chem. Soc.*, 2002, **124**, 4487.
175. N.E. Gruhn, A. Rai-Chaudhuri, S.K. Renshaw, J.A. Gladysz, H.J. Jiao, J. Seyler and A. Igau, *J. Am. Chem. Soc.*, 2002, **124**, 1417.
176. J.K. Law, H. Mellows and D.M. Heinekey, *J. Am. Chem. Soc.*, 2002, **124**, 1024.
177. Z.M. Hu, R.J. Boyd and H. Nakatsuji, *J. Am. Chem. Soc.*, 2002, **124**, 2664.
178. M. Catellani, C. Mealli, E. Motti, P. Paoli, E. Perez-Carreno and P.S. Pregosin, *J. Am. Chem. Soc.*, 2002, **124**, 4336.
179. S.Y. Yang, X.Y. Li and Y.Z. Huang, *J. Organomet. Chem.*, 2002, **658**, 9.
180. F. Paul, K. Costuas, I. Ledoux, S. Deveau, J. Zyss, J.F. Halet and C. Lapinte, *Organometallics*, 2002, **21**, 5229.
181. J.A.S. Howell, P.C. Yates and N. Fey, *Organometallics*, 2002, **21**, 5272.
182. H. Aneetha, M. Jimenez-Tenorio, M.C. Puerta, P. Valerga, V.N. Sapunov, R. Schmid, K. Kirchner and K. Mereiter, *Organometallics*, 2002, **21**, 5334.
183. A.M. Gillespie, G.R. Morello and D.P. White, *Organometallics*, 2002, **21**, 3913.
184. D.L. Cedenio and E. Weitz, *J. Am. Chem. Soc.*, 2002, **124**, 12857.
185. T. Strassner, M. Muehlhofer and S. Grasser, *J. Organomet. Chem.*, 2002, **641**, 121.
186. G. Frison and H. Grutzmacher, *J. Organomet. Chem.*, 2002, **643**, 285.
187. T.P.M. Goumans, A.W. Ehlers, M.J.M. Vlaar, S.J. Strand and K. Lammertsma, *J. Organomet. Chem.*, 2002, **643**, 369.
188. A. Galindo, M. Gomez, P. Gomez-Sal, A. Martin, D. del Rio and F. Sanchez, *Organometallics*, 2002, **21**, 293.
189. J.J. Carbo, P. Crochet, M.A. Esteruelas, Y. Jean, A. Lledos, A.M. Lopez and E. Onate, *Organometallics*, 2002, **21**, 305.
190. Y.A. Borisov, M.I. Rybinskaya, Y.S. Nekrasov, A.Z. Kreindlin, A.A. Kamyshova and P.V. Petrovskii, *J. Organomet. Chem.*, 2002, **645**, 87.
191. D. Weiss, M. Winter, K. Merz, A. Knufer, R.A. Fischer, N. Frohlich and G. Frenking, *Polyhedron*, 2002, **21**, 535.
192. J.A. Chamizo, J. Morgado, M. Castro and S. Bernes, *Organometallics*, 2002, **21**, 5428.
193. M.B. Wells, J.E. McConathy, P.S. White and J.L. Templeton, *Organometallics*, 2002, **21**, 5007.
194. R. Blom and O. Swang, *Eur. J. Inorg. Chem.*, 2002, **2**, 411.
195. M. Kaupp, T. Kopf, A. Murso, D. Stalke, C. Strohmman, J.R. Hanks, F.G.N. Cloke and P.B. Hitchcock, *Organometallics*, 2002, **21**, 5021.
196. A. Vega, V. Calvo, E. Spodine, A. Zarate, V. Fuenzalida and J.Y. Saillard, *Inorg. Chem.*, 2002, **41**, 3389.
197. C. Graiff, A. Ienco, C. Massera, C. Mealli, G. Predieri, A. Tiripicchio and F. Ugozzoli, *Inorg. Chim. Acta*, 2002, **330**, 95.
198. D.L. Bryce and R.E. Wasylshen, *Phys. Chem. Chem. Phys.*, 2002, **4**, 3591.
199. R.D. Adams, B. Qu, M.D. Smith and T.A. Albright, *Organometallics*, 2002, **21**, 2970.
200. A.D. Burrows, N. Carr, M. Green, J.M. Lynam, M.F. Mahon, M. Murray, B. Kiran,

- N.T. Nguyen and C. Jones, *Organometallics*, 2002, **21**, 3076.
201. S. Grigoleit, A. Alijah, A.B. Rozhenko, R. Streubel and W.W. Schoeller, *J. Organomet. Chem.*, 2002, **643**, 223.
202. H.G. Raubenheimer, M.W. Esterhuysen, A. Timoshkin, Y. Chen and G. Frenking, *Organometallics*, 2002, **21**, 3173.
203. M. Niehues, G. Erker, G. Kehr, P. Schwab, R. Frohlich, O. Blacque and H. Berke, *Organometallics*, 2002, **21**, 2905.
204. A. Marrone and N. Re, *Organometallics*, 2002, **21**, 3562.
205. G. Aullon and S. Alvarez, *Organometallics*, 2002, **21**, 2627.
206. J.C. Gordon, G.R. Giesbrecht, D.L. Clark, P.J. Hay, D.W. Keogh, R. Poli, B.L. Scott and J.G. Watkin, *Organometallics*, 2002, **21**, 4726.
207. E.D. Jemmis, A.K. Phukan and K.T. Giju, *Organometallics*, 2002, **21**, 2254.
208. J.M. Tanski and G. Parkin, *Organometallics*, 2002, **21**, 587.
209. D. del Rio and A. Galindo, *J. Organomet. Chem.*, **655**, 16.
210. P. Belanzoni, N. Re and A. Sgamellotti, *J. Organomet. Chem.*, 2002, **656**, 156.
211. D. Moigno, B. Callejas-Gaspar, J. Gil-Rubio, H. Werner and W. Kiefer, *J. Organomet. Chem.*, 2002, **661**, 181.
212. S. Maricic and T. Frejd, *J. Org. Chem.*, 2002, **67**, 7600.
213. G.A. Bogdanovic, A.S.D. Bire and S.D. Zaric, *Eur. J. Inorg. Chem.*, 2002, **7**, 1599.
214. K.B. Lipkowitz, C.A. D'Hue, T. Sakamoto and J.N. Stack, *J. Am. Chem. Soc.*, 2002, **124**, 14255.
215. J. van Slageren, A. Klein and S. Zalis, *Coord. Chem. Rev.*, 2002, **230**, 193.
216. B.H. Kim and C.R.F. Lund, *J. Mol. Catal. A – Chem.*, 2002, **188**, 173.
217. M. Buhl, F.T. Mauschick, *J. Organomet. Chem.*, 2002, **646**, 126.
218. Z.T. Xu, K. Vanka, T. Firman, A. Michalak, E. Zurek, C.B. Zhu and T. Ziegler, *Organometallics*, 2002, **21**, 2444.
219. E. Zurek and T. Ziegler, *Organometallics*, 2002, **21**, 83.
220. A. Michalak and T. Ziegler, *J. Am. Chem. Soc.*, 2002, **124**, 7519.
221. G. Talarico, A.N.J. Blok, T.K. Wo and L. Cavallo, *Organometallics*, 2002, **21**, 4939.
222. S. Bhaduri, S. Mukhopadhyay and S.A. Kulkarni, *J. Organomet. Chem.*, 2002, **654**, 132.
223. A. Zeller and T. Strassner, *Organometallics*, 2002, **21**, 4950.
224. T. Tomita, T. Takahama, M. Sugimoto and S. Sakaki, *Organometallics*, 2002, **21**, 4138.
225. E. Ruba, K. Mereiter, R. Schmid, V.N. Sapunov, K. Kirchner, H. Schottenberger, M.J. Calhorda and L.F. Veiros, *Chem. Eur. J.*, 2002, **8**, 3948.
226. H. von Schenck, B. Akermark and M. Svensson, *Organometallics*, 2002, **21**, 2248.
227. M. Widhalm, U. Nettekoven, H. Kalchhauser, K. Mereiter, M.J. Calhorda and V. Felix, *Organometallics*, 2002, **21**, 315.
228. N. Sandig and W. Koch, *Organometallics*, 2002, **21**, 1861.
229. M.J. Young, C.C.M. Ma and C. Ting, *Russ. J. Coord. Chem.*, 2002, **28**, 25.
230. I. Shiina, K. Konishi and Y. Kuramoto, *Chem. Lett.*, 2002, **31**, 164.
231. Z.W. Liu, M. Torrent and K. Morokuma, *Organometallics*, 2002, **21**, 1056.
232. S. Tobisch, *Chem. - Eur. J.*, 2002, **8**, 4756.
233. V.R. Jensen and K.J. Borve, *Chem. Commun.*, 2002, 542.
234. H.Q. Yang, Y.Q. Chen, C.W. Hu, M.C. Gong, H.R. Hu, A.M. Tian and N.B. Wong, *Chem. Phys. Lett.*, 2002, **355**, 233.
235. D.Y. Hwang and A.M. Mebel, *Chem. Phys. Lett.*, 2002, **365**, 140.
236. S.M. Ng, C. Zhao and Z.Y. Lin, *J. Organomet. Chem.*, 2002, **662**, 120.
237. M. Jakt, L. Johannissen, H.S. Rzepa, D.A. Widdowson and R. Wilhelm, *J. Chem. Soc.-Perkin Trans. 2*, 2002, 576.

238. K. Yoshizawa, *Coord. Chem. Rev.*, 2002, **226**, 251.
239. T. Matsubara and K. Hirao, *Organometallics*, 2002, **21**, 4482.
240. E. Sicilia and N. Russo, *J. Am. Chem. Soc.*, 2002, **124**, 1471.
241. G. Ferrando-Miguel, H. Gerard, O. Eisenstein and K.G. Caulton, *Inorg. Chem.*, 2002, **41**, 6440.
242. K. Krogh-Jespersen, M. Czerw, N. Summa, K.B. Renkema, P.D. Achord and A.S. Goldman, *J. Am. Chem. Soc.*, 2002, **124**, 11404.
243. D.G. Gusev and A.J. Lough, *Organometallics*, 2002, **21**, 5091.
244. R.K. Szilagy, D.G. Musaev and K. Morokuma, *Organometallics*, 2002, **21**, 555.
245. M.A. Iron, H.C. Lo, J.M.L. Martin and E. Keinan, *J. Am. Chem. Soc.*, 2002, **124**, 7041.
246. S.H. Liu, X. Huang, Z.Y. Lin, C.P. Lau and G.C. Jia, *Eur. J. Inorg. Chem.*, 2002, **7**, 1697.
247. J.P. Rourke, G. Stringer, P. Chow, R.J. Deeth, D.S. Yufit, J.A.K. Howard and T.B. Marder, *Organometallics*, 2002, **21**, 429.
248. F. Nunzi, A. Sgamellotti and N. Re, *Organometallics*, 2002, **21**, 2219.
249. E. Nakamura, N. Yoshikai and M. Yamanaka, *J. Am. Chem. Soc.*, 2002, **124**, 7181.
250. J.R. Fulton, S. Sklenak, M.W. Bouwkamp and R.G. Bergman, *J. Am. Chem. Soc.*, 2002, **124**, 4722.
251. D.G. Musaev, H. Basch and K. Morokuma, *J. Am. Chem. Soc.*, 2002, **124**, 4135.
252. T.R. Cundari, T.R. Klinckman and P.T. Wolczanski, *J. Am. Chem. Soc.*, 2002, **124**, 1481.
253. I. Atheaux, F. Delpech, B. Donnadiou, S. Sabo-Etienne, B. Chaudret, K. Hussein, J.C. Barthelat, T. Braun, S.B. Duckett and R.N. Perutz, *Organometallics*, 2002, **21**, 5347.
254. D.S. McGuinness, B.F. Yates and K.L.J. Cavell, *Organometallics*, 2002, **21**, 5408.
255. X.H. Wan, X.J. Wang, Y. Luo, S. Takami, M. Kubo and A. Miyamoto, *Organometallics*, 2002, **21**, 3703.
256. S. Sakaki, M. Sumimoto, M. Fukuhara, M. Sugimoto, H. Fujimoto and S. Matsuzaki, *Organometallics*, 2002, **21**, 3788.
257. T. Matsubara and K. Hirao, *Organometallics*, 2002, **21**, 2662.
258. M.N. Jagadeesh, W. Thiel, J. Kohler and A. Fehn, *Organometallics*, 2002, **21**, 2076.
259. D.J. Nielsen, A.M. Magill, B.F. Yates, K.J. Cavell, B.W. Skelton and A.H. White, *Chem. Commun.*, 2002, 2500.
260. T. Matsubara and K. Hirao, *J. Am. Chem. Soc.*, 2002, **124**, 679.
261. K.L. Tan, R.G. Bergman and J.A. Ellman, *J. Am. Chem. Soc.*, 2002, **124**, 3202.
262. J. Kua, X. Xu, R.A. Periana and W.A. Goddard, *Organometallics*, 2002, **21**, 511.
263. W.R. Thiel and K. Krohn, *Chem. – Eur. J.*, 2002, **8**, 1049.
264. S. Fantacci, F. De Angelis, A. Sgamellotti and N. Re, *Organometallics*, 2002, **21**, 4090.
265. F. De Angelis, A. Sgamellotti and N. Re, *Organometallics*, 2002, **21**, 2715.
266. F. De Angelis, A. Sgamellotti and N. Re, *Organometallics*, 2002, **21**, 2036.
267. S.K. Goh and D.S. Marynick, *Organometallics*, 2002, **21**, 2262.
268. H.Z. Li, K.Q. Yu, E.J. Watson, K.L. Virkaitis, J.S. D'Acchioli, G.B. Carpenter, D.A. Sweigart, P.T. Czech, K.R. Overly and F. Coughlin, *Organometallics*, 2002, **21**, 1262.
269. S.A. Macgregor and E. Wenger, *Organometallics*, 2002, **21**, 1278.
270. K.P. Gable, P. Chuawong and A.F.T. Yokochi, *Organometallics*, 2002, **21**, 929.
271. V. Cadierno, S. Conejero, M.P. Gamasa, J. Gimeno and M.A. Rodriguez, *Organometallics*, 2002, **21**, 203.
272. A. Fuchs, D. Gudat, M. Nieger, O. Schmidt, M. Sebastian, L. Nyulaszi and E.

- Niecke, *Chem. – Eur. J.*, 2002, **8**, 2188.
273. G. Giorgi, F. De Angelis, N. Re and A. Sgamellotti, *Chem. Phys. Lett.*, 2002, **364**, 87.
274. F. Schaper, A. Geyer and H.H. Brintzinger, *Organometallics*, 2002, **21**, 473.
275. L. Perrin, L. Maron and O. Eisenstein, *Inorg. Chem.*, 2002, **41**, 4355.
276. O.V. Ozerov, H.F. Gerard, L.A. Watson, J.C. Huffman and K.G. Caulton, *Inorg. Chem.*, 2002, **41**, 5615.
277. A. Bottoni, A.P. Higueroelo and G.P. Miscione, *J. Am. Chem. Soc.*, 2002, **124**, 5506.
278. M. Cui, W. Adam, J.H. Shen, X.M. Luo, X.J. Tan, K.X. Chen, R.Y. Ji and H.L. Jiang, *J. Org. Chem.*, 2002, **67**, 1427.
279. D. Liu and Z.Y. Lin, *Organometallics*, 2002, **21**, 4750.
280. N. Lopez and J.K. Norskov, *J. Am. Chem. Soc.*, 2002, **124**, 11262.
281. Y. Musashi and S. Sakaki, *J. Am. Chem. Soc.*, 2002, **124**, 7588.
282. S.H. Liu, S.M. Ng, T.B. Wen, Z.Y. Zhou, Z.Y. Lin, C.P. Lau and G. Jia, *Organometallics*, 2002, **21**, 4281.
283. G. Ferrando-Miguel, J.N. Coalter, H. Gerard, J.C. Huffman, O. Eisenstein and K.G. Caulton, *New. J. Chem.*, 2002, **26**, 687.
284. V. Branchadell, M. Moreno-Manas and R. Pleixats, *Organometallics*, 2002, **21**, 2407.
285. S.Y. Kang, T. Yamabe, A. Naka, M. Ishikawa and K. Yoshizawa, *Organometallics*, 2002, **21**, 150.
286. T. Hascall, M.H. Baik, B.A. Bridgewater, J.H. Shin, D.G. Churchill, R.A. Friesner and G. Parkin, *Chem. Commun.*, 2002, 2644.
287. D.V. Yandulov and K.G. Caulton, *New. J. Chem.*, 2002, **26**, 498.
288. S.E. Vyboishchikov, M. Buhl and W. Thiel, *Chem. - Eur. J.*, 2002, **8**, 3962.
289. B.F. Straub, *J. Am. Chem. Soc.*, 2002, **124**, 14195.
290. C.Y. Zhao, D.Q. Wang and D.L. Phillips, *J. Am. Chem. Soc.*, 2002, **124**, 12903.
291. A.S. Borovik and A.R. Barron, *J. Am. Chem. Soc.*, 2002, **124**, 3743.
292. M. Aresta, A. Dibenedetto, I. Papai and G. Schubert, *Inorg. Chim. Acta.*, 2002, **334**, 294.
293. S. Tobisch and T. Ziegler, *J. Am. Chem. Soc.*, 2002, **124**, 13290.
294. S. Tobisch and T. Ziegler, *J. Am. Chem. Soc.*, 2002, **124**, 4881.
295. D.V. Deubel and T. Ziegler, *Organometallics*, 2002, **21**, 4432.
296. D.V. Deubel and T. Ziegler, *Organometallics*, 2002, **21**, 1603.
297. V.P. Ananikov, D.G. Musaev and K. Morokuma, *J. Am. Chem. Soc.*, 2002, **124**, 2839.
298. T. Matsubara and K. Hirao, *Organometallics*, 2002, **21**, 1697.
299. Y.B. Fan and M.B. Hall, *J. Am. Chem. Soc.*, 2002, **124**, 12076.
300. F. Teply, I.G. Stara, I. Stary, A. Kollarovic, D. Saman, L. Rulisek and P. Fiedler, *J. Am. Chem. Soc.*(184) 2002, **124**, 9175.
301. L. Cavallo, *J. Am. Chem. Soc.*, 2002, **124**, 8965.
302. Y.H. Sheng, D.G. Musaev, K.S. Reddy, F.E. McDonald and K. Morokuma, *J. Am. Chem. Soc.*, 2002, **124**, 4149.
303. M.H. Chisholm, E.R. Davidson, M. Pink and K.B. Quinlan, *Chem. Commun.*, 2002, 2770.
304. L.R. Domingo, J. Andres and C.N. Alves, *Eur. J. Org. Chem.*, 2002, **15**, 2557.
305. T. Ikeno, I. Iwakura, S. Yabushita and T. Yamada, *Org. Lett.*, 2002, **4**, 517.